

# <sup>1</sup> The Evolution of Siphonophore Tentilla as Specialized Tools for Prey Capture

<sup>3</sup> Alejandro Damian-Serrano<sup>1,‡</sup>, Steven H.D. Haddock<sup>2</sup>, Casey W. Dunn<sup>1</sup>

<sup>4</sup> <sup>1</sup> Yale University, Department of Ecology and Evolutionary Biology, 165 Prospect St.,  
<sup>5</sup> New Haven, CT 06520, USA

<sup>6</sup> <sup>2</sup> Monterey Bay Aquarium Research Institute, 7700 Sandholdt Rd., Moss Landing, CA  
<sup>7</sup> 95039, USA

<sup>8</sup> <sup>‡</sup> Corresponding author: Alejandro Damian-Serrano, email: alejandro.damianserrano@  
<sup>9</sup> yale.edu

## <sup>10</sup> Abstract

<sup>11</sup> Predators have evolved dedicated body parts to capture and subdue prey. As different  
<sup>12</sup> predators specialize on distinct prey taxa, their tools for prey capture diverge into a variety  
<sup>13</sup> of adaptive forms. Studying the evolution of predation is greatly facilitated by a predator  
<sup>14</sup> clade with structures used exclusively for prey capture that present significant morphological  
<sup>15</sup> variation. Siphonophores, a clade of colonial cnidarians, satisfy these criteria particularly  
<sup>16</sup> well, capturing prey with their tentilla (tentacle side branches). Earlier work has shown that  
<sup>17</sup> extant siphonophore diets correlate with the different morphologies and sizes of their tentilla  
<sup>18</sup> and nematocysts. We hypothesize that evolutionary specialization on different prey types has  
<sup>19</sup> driven the phenotypic evolution of these characters. To test this hypothesis, we: (1) measured  
<sup>20</sup> multiple morphological traits from fixed siphonophore specimens using microscopy and high  
<sup>21</sup> speed video techniques, (2) built a phylogenetic tree of 45 species, and (3) characterized  
<sup>22</sup> the evolutionary associations between siphonophore nematocyst characters and prey type  
<sup>23</sup> data from the literature. Our results show that siphonophore tentillum structure has strong  
<sup>24</sup> evolutionary associations with prey type and size specialization, and suggest that shifts  
<sup>25</sup> between prey-type specializations are linked to shifts in tentillum and nematocyst size and

<sup>26</sup> shape. In addition, we generated hypotheses about the diets of understudied siphonophore  
<sup>27</sup> species based on these characters. Thus, the evolutionary history of tentilla shows that  
<sup>28</sup> siphonophores are an example of ecological niche diversification via morphological innovation  
<sup>29</sup> and evolution. This study contributes to understanding how morphological evolution has  
<sup>30</sup> shaped present-day oceanic food-webs.

<sup>31</sup> **Keywords**

<sup>32</sup> Siphonophores, tentilla, nematocysts, predation, specialization, character evolution

<sup>33</sup>

<sup>34</sup> Most animal predators have characteristic biological tools that they use to capture and  
<sup>35</sup> subdue prey. Raptors have claws and beaks, snakes have fangs, wasps have stingers, and  
<sup>36</sup> cnidarians have nematocyst-laden tentacles. The functional morphology of these structures  
<sup>37</sup> tend to be finely attuned to their ability to successfully capture specific prey (Schmitz  
<sup>38</sup> 2017). Long-term adaptive evolution in response to the defense mechanisms of the prey (*e.g.*  
<sup>39</sup> avoidance, escape, protective barriers) leads to modifications that can counter those defenses  
<sup>40</sup> The more specialized the diet of a predator is, the more specialized its tools need to be to  
<sup>41</sup> meet the specific challenges posed by the prey. Understanding the relationships between  
<sup>42</sup> predatory specializations and morphological specializations is necessary to contextualize the  
<sup>43</sup> phenotypic diversity of predators, and to quantify the importance of ecological diversification  
<sup>44</sup> in generating this diversity.

<sup>45</sup> Siphonophores (Cnidaria : Hydrozoa) are a clade of organisms bearing modular structures  
<sup>46</sup> that are exclusively used for prey capture: the tentilla (Fig. 1). These present a significant  
<sup>47</sup> morphological variation across species (Mapstone 2014) (Fig. 2), which makes it ideal to study  
<sup>48</sup> the relationships between functional traits and prey specialization. A siphonophore is a colony  
<sup>49</sup> bearing many feeding polyps (Fig. 1), each with a single tentacle, which branches into several  
<sup>50</sup> tentilla carrying the functional cnidocytes (specialized neural cells carrying nematocysts,

51 the stinging capsules). Unlike most other cnidarians, siphonophores carry their tentacle  
52 nematocysts in extremely complex and organized batteries (Skaer 1988), built into their  
53 tentilla. While nematocyst batteries and clusters in other cnidarians are simple static scaffolds  
54 for cnidocytes, siphonophore tentilla have their own reaction mechanism, triggered upon  
55 encounter with prey. When it fires, a tentillum undergoes an extremely fast conformational  
56 change that wraps it around the prey, maximizing the surface area of contact for nematocysts  
57 to fire on the prey (Mackie et al. 1987). In addition, some species have elaborate fluorescent  
58 and bioluminescent lures on their tentilla to attract prey with aggressive mimicry (Purcell  
59 1980; Haddock et al. 2005; Haddock and Dunn 2015).

60 Many siphonophore species inhabit the deep pelagic ocean, which spans from ~200m to  
61 the oceanic seafloor. This habitat has fairly homogeneous physical conditions and stable  
62 abundances of zooplanktonic animals (Robison 2004). With a relatively predictable prey  
63 availability, ecological theory would predict evolution to drive coexisting siphonophore  
64 lineages towards specialization, increasing their feeding efficiencies and reducing interspecific  
65 competition (Hardin 1960; Hutchinson 1961). If this prediction holds true, we expect the prey  
66 capture apparatus morphologies of siphonophores to diversify with the evolution of increased  
67 specialization on a variety of prey types in different siphonophore lineages.

68 Coexisting siphonophores feeding on the same planktonic community may have substantial  
69 niche overlap and compete for prey resources. Traditional ecological coexistence theory  
70 (Simpson 1944) predicts that competition between species would select for increasing ecological  
71 specialization. This specialization is often thought to be an evolutionary ‘dead end’, meaning  
72 that specialized lineages are unlikely to evolve into generalists or to shift the resource for  
73 which they are specialized (Futuyma and Moreno 1988). However, recent studies have found  
74 that interspecific competition can favor the evolution of resource generalism (Stireman-III  
75 2005; Johnson et al. 2009) and resource switching (Hoberg and Brooks 2008). Here we  
76 examine three alternative hypotheses on siphonophore trophic specialization: (1) predatory  
77 specialists evolved from generalist ancestors; (2) predatory specialists evolved from ancestral

78 predatory specialists which specialized on a different resource, switching their primary prey  
79 type; and (3) predatory generalists evolved from specialist ancestors.

80 The study of siphonophore tentilla and diets has been limited in the past due to the  
81 inaccessibility of their oceanic habitat and the difficulties associated with the collection of  
82 fragile siphonophores. Thus, the morphological diversity of tentilla has only been characterized  
83 for a few taxa, and their evolutionary history remains largely unexplored. Contemporary  
84 underwater sampling technology provides an unprecedented opportunity to explore the trophic  
85 ecology (Choy et al. 2017) and functional morphology (Costello et al. 2015) of siphonophores.  
86 In addition, well-supported phylogenies based on molecular data are now available for these  
87 organisms (Munro et al. 2018). These advances allow for the examination of relationships  
88 between modern siphonophore form, function, and ecology, as well as reconstructing their  
89 evolutionary history.

90 The few pioneering studies that have addressed the relationships between tentilla and  
91 diet suggest that siphonophores are a robust system for the study of predatory specialization  
92 via morphological diversification. (Purcell 1984) and (Purcell and Mills 1988) showed clear  
93 relationships between diet, tentillum, and nematocyst characters in co-occurring epipelagic  
94 siphonophores. These correlations, while studied for a small subset of extant epipelagic  
95 siphonophore species, might be generalizable to all siphonophores. We hypothesize that  
96 these relationships reflect correlated evolution between prey selection and tentillum (and  
97 nematocyst) traits. Furthermore, we hypothesize that with an extensive characterization of  
98 tentilla morphology, we can generate hypotheses about the diets of understudied siphonophore  
99 species. In addition, our study design allows us to address other interesting questions about  
100 the morphology and evolution of these unique structures. In particular, we aim to address  
101 the evolutionary origins of giant tentilla, the phenotypic integration of tentilla, the evolution  
102 of the extreme shapes of siphonophore haploneme nematocysts (Thomason 1988), and the  
103 mechanical implications of tentillum morphologies on cnidoband discharge.

104 In this study, we characterize the morphological diversity of tentilla and their nematocysts

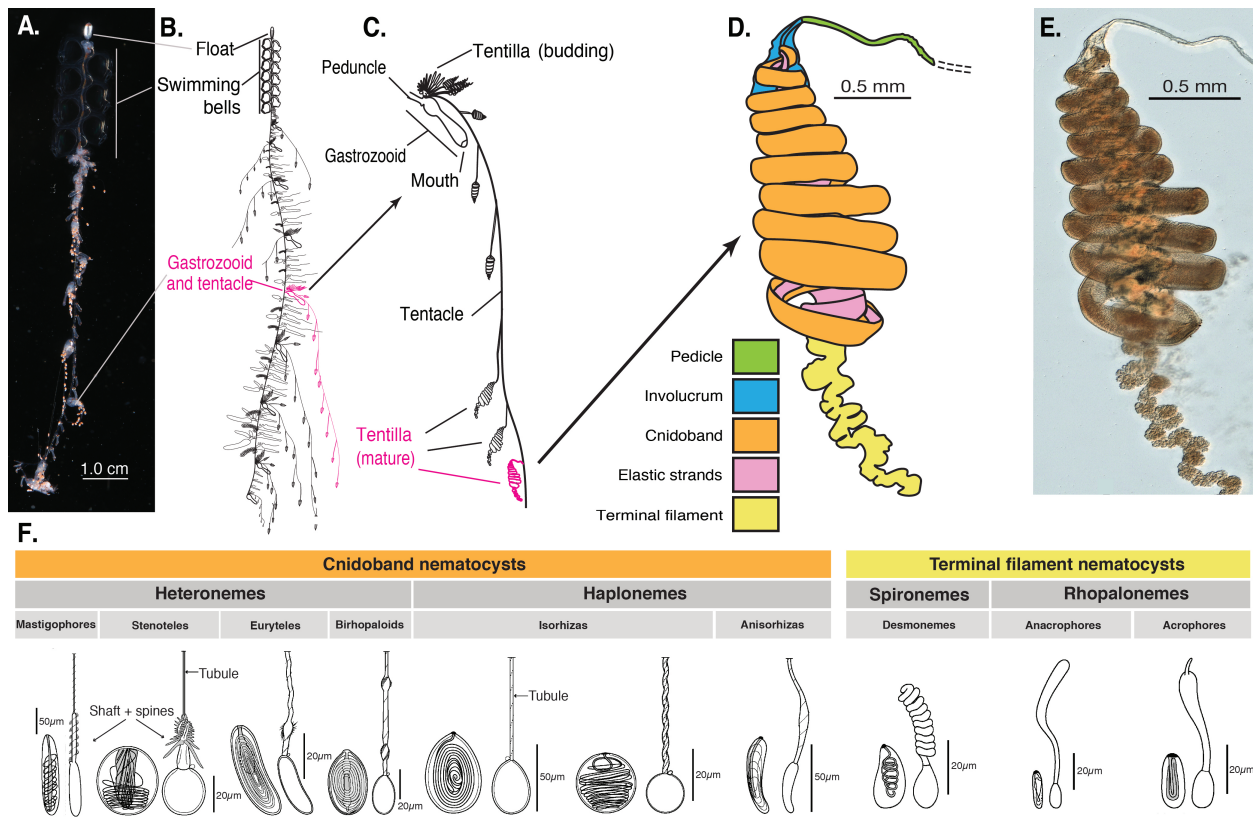


Figure 1: Siphonophore anatomy. A - *Nanomia* sp. siphonophore colony (photo by Catriona Munro). B,C - Illustration of a *Nanomia* colony, gastrozooid, and tentacle (by Freya Goetz). D - *Nanomia* sp. Tentillum illustration and main parts. E - Transmission micrograph of the tentillum illustrated in D. F - Nematocyst types (illustration reproduced with permission from Mapstone 2014), hypothesized homologies, and locations in the tentillum. Undischarged to the left, discharged to the right.

105 across a broad variety of shallow and deep sea siphonophore species using modern imaging  
 106 technologies, we expand the phylogenetic tree of siphonophores by combining a broad taxon  
 107 sampling of ribosomal gene sequences with a transcriptome-based backbone tree, and we  
 108 explore the evolutionary histories and correlations among diet, tentillum, and nematocyst  
 109 characters.

## 110 Methods

111 *Tentillum morphology* – The morphological work was carried out on siphonophore specimens  
 112 fixed in 4% formalin from the Yale Peabody Museum Invertebrate Zoology (YPM-IZ) collection

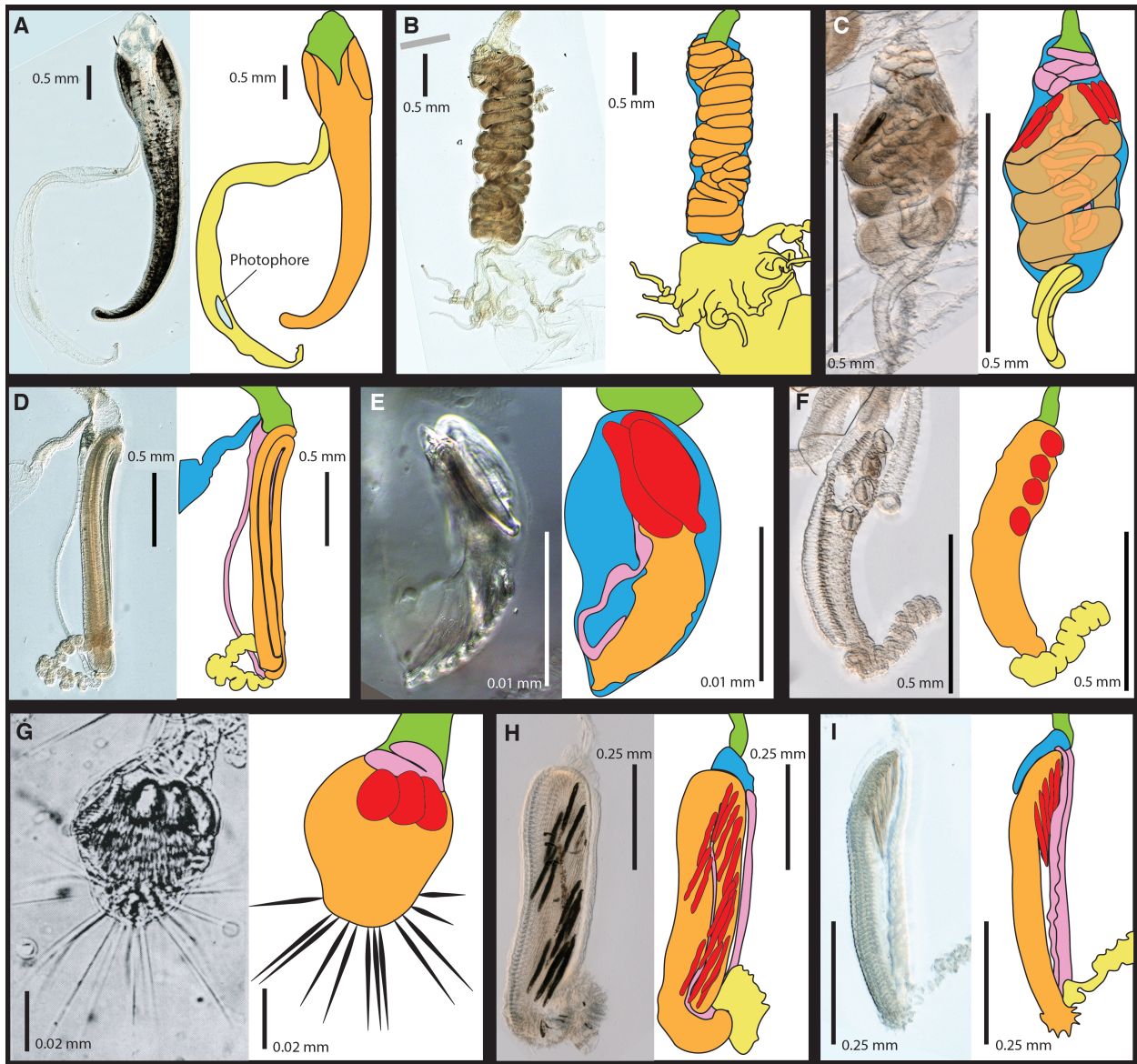


Figure 2: Tentillum diversity plate. The illustrations delineate the pedicle (green), involucrum (blue), cnidoband (orange), elastic strands (pink), terminal structures (yellow). Heteroneme nematocysts (stenoteles in C,E,F,G and mastigophores in H,I) are depicted in red for some species. A - *Erenna laciniata*, 10x. B - *Lychnagalma utricularia*, 10x. C - *Agalma elegans*, 10x. D - *Resomia ornicephala*, 10x. E - *Frillagalma vityazi*, 20x. F - *Bargmannia amoena*, 10x. G - *Cordagalma* sp., reproduced from Carré 1968. H - *Lilyopsis fluoracantha*, 20x. I - *Abylopsis tetragona*, 20x.

113 (accession numbers in Appendix 1). These specimens were collected intact across many years  
114 of fieldwork expeditions, using blue-water diving (Haddock and Heine 2005), remotely  
115 operated vehicles (ROVs), and human-operated submersibles. Tentacles were dissected  
116 from non-larval gastrozooids, sequentially dehydrated into 100% ethanol, cleared in methyl  
117 salicylate, and mounted into slides with Canada Balsam or Permount mounting media. The  
118 slides were imaged as tiled z-stacks using differential interference contrast (DIC) on an  
119 automated stage at YPM-IZ (with the assistance of Daniel Drew and Eric Lazo-Wasem) and  
120 with laser point confocal microscopy using a 488 nm Argon laser that excited autofluorescence  
121 in the tissues. Thirty characters (defined in Appendix 2) were measured using Fiji (Collins  
122 2007; Schindelin et al. 2012). We did not measure the lengths of contractile structures  
123 (terminal filaments, pedicles, gastrozooids, and tentacles), since they are too variable to  
124 quantify. We measured at least one specimen for 96 different species (Appendix 3, Fig.  
125 3). Of these, we selected 38 focal species across clades based on specimen availability and  
126 phylogenetic representation. Three to five tentacle specimens from each one of these selected  
127 species were measured to capture intraspecific variation.

128 In order to observe the discharge behavior of different tentilla, we recorded high speed  
129 footage (1000-3000 fps) of tentillum and nematocyst discharge by live siphonophore specimens  
130 (26 species) using a Phantom Miro 320S camera mounted on a stereoscopic microscope. We  
131 mechanically elicited tentillum and nematocyst discharge using a fine metallic pin. We used  
132 the Phantom PCC software to analyze the footage. For the 10 species recorded, we measured  
133 total cnidoband discharge time (ms), heteroneme filament length ( $\mu\text{m}$ ), and discharge speeds  
134 ( $\text{mm/s}$ ) for cnidoband, heteronemes, haplonemes, and heteroneme shafts when possible (data  
135 in Appendix 4).

136 *Siphonophore phylogeny* – The phylogenetic analysis included 55 siphonophore species  
137 and 6 outgroup cnidian species (*Clytia hemisphaerica*, *Hydra circumcincta*, *Ectopleura*  
138 *dumortieri*, *Porpita porpita*, *Velella velella*, *Staurocladia wellingtoni*). The gene sequences  
139 we used in this study are available online (accession numbers in Appendix 5). Some of

the sequences we used were accessioned in (Dunn et al. 2005), and others we extracted from the transcriptomes in (Munro et al. 2018). Two new 16S sequences for *Frillagalma vityazi* (MK958598) and *Thermopalia* sp. (MK958599) sequenced by Lynne Christianson were included and accessioned to NCBI. We aligned these sequences using MAFFT (Katoh et al. 2002) (alignments available in Dryad). We inferred a Maximum Likelihood (ML) phylogeny (Appendix 6) from 16S and 18S ribosomal rRNA genes using IQTree (Nguyen et al. 2014) with 1000 bootstrap replicates (iqtree -s alignment.fa -nt AUTO -bb 1000). We used ModelFinder (Kalyaanamoorthy et al. 2017) implemented in IQTree v1.5.5. to assess relative model fit. ModelFinder selected GTR+R4 for having the lowest Bayesian Information Criterion score. Additionally, we inferred a Bayesian tree with each gene as an independent partition in RevBayes (Höhna et al. 2016) (Appendix 7 and 9), which was topologically congruent with the unconstrained ML tree. The *alpha* priors were selected to minimize prior load in site variation.

Given the broader sequence sampling of the transcriptome phylogeny, we ran constrained inferences (using both ML and Bayesian timetree approaches, which produced fully congruent topologies (Appendix 6 and 7)) after fixing the 5 nodes that were incongruent with the topology of the consensus tree in (Munro et al. 2018). This topology was then used to inform a Bayesian relaxed molecular clock time-tree in RevBayes, using a birth-death process (sampling probability calculated from the known number of described siphonophore species) to generate ultrametric branch lengths (Appendix 8). Scripts available in Appendix 9.

*Feeding ecology* – We extracted categorical diet data for different siphonophore species from published sources, including seminal papers (Biggs 1977; Purcell 1981, 1984; Andersen 1981; Mackie et al. 1987; Pugh and Youngbluth 1988; Bardi and Marques 2007), and ROV observation data (Hissmann 2005; Choy et al. 2017) with the assistance of Elizabeth Hetherington and Anela Choy (Appendix 10). We removed the gelatinous prey observations for *Praya dubia* eating a ctenophore and a hydromedusa, and for *Nanomia* sp. eating *Aegina*, since we believe these are rare events that have a much larger probability of being detected by ROV

methods than their usual prey, and it is not clear whether the medusae were attempting to prey upon the siphonophores. Personal observations on feeding (from SHDH, CAC, and Philip Pugh) were also included for *Resomia ornicephala*, *Lychnagalma utricularia*, *Bargmannia amoena*, *Erenna richardi*, *Erenna laciniata*, *Erenna sirena*, and *Apolemia rubriversa*. In order to detect coarse-level patterns in the feeding habits, the data were merged into feeding guilds. The feeding guilds described here are: small-crustacean specialist (feeding mainly on copepods and ostracods), large crustacean specialist (feeding on large decapods, mysids, or krill), fish specialist (feeding mainly on actinopterygian larvae, juveniles, or adults), gelatinous specialist (feeding mainly on other siphonophores, medusae, ctenophores, salps, and/or doliolids), and generalist (feeding on a combination of the aforementioned taxa, without favoring any one prey group). These were selected to minimize the number of categories while keeping the most different types of prey separate. We extracted copepod prey length data from (Purcell 1984). To calculate specific prey selectivities, we extracted quantitative diet and zooplankton composition data from (Purcell 1981), matched each diet assessment to each prey field quantification by site, calculated Ivlev's electivity indices (Jacobs 1974), and averaged those by species (Appendix 11).

*Statistical analyses* – For subsequent comparative analyses, we removed species present in the tree but not represented in the morphology data, and *vice versa*. Although we measured specimens labeled as *Nanomia bijuga* and *Nanomia cara*, we are not confident in some of the species-level identifications, and some specimens were missing diagnostic zooids. Thus, we decided to collapse these into a single taxonomic concept (*Nanomia* sp.). All *Nanomia* sp. observations were matched to the phylogenetic position of *Nanomia bijuga* in the tree. We carried out all phylogenetic comparative statistical analyses in the programming environment R (Team 2017), using the bayesian ultrametric species tree (Fig. 4), and incorporating intraspecific variation estimated from the specimen data as standard error (Appendix 3). R scripts available in Dryad. For each character (or character pair) analyzed, we removed species with missing data and reported the number of taxa included. We tested each character

<sup>194</sup> for normality using the Shapiro-Wilk test (Shapiro and Wilk 1965), and log-transformed  
<sup>195</sup> those that were non-normal.

<sup>196</sup> We fitted different models generating the observed data distribution given the phylogeny  
<sup>197</sup> for each continuous character using the function `fitContinuous` in the R package *geiger*  
<sup>198</sup> (Harmon et al. 2007). The models compared were the white noise (WN; non-phylogenetic  
<sup>199</sup> model that assumes all values come from a single normal distribution with no covariance  
<sup>200</sup> structure among species), the Brownian Motion (BM) model of neutral divergent evolution  
<sup>201</sup> (Martins 1996), the Early Burst (EB) model of decreasing rate of evolutionary change (Harmon  
<sup>202</sup> et al. 2010), and the Ornstein-Uhlenbeck (OU) model of stabilizing selection around a fitted  
<sup>203</sup> optimum state (Uhlenbeck and Ornstein 1930; Butler and King 2004). We then ranked the  
<sup>204</sup> models in order of increasing parametric complexity (WN,BM,EB,OU), and compared the  
<sup>205</sup> corrected Akaike Information Criterion (AICc) support scores (Sugiura 1978) to the lowest  
<sup>206</sup> (best) score, using a cutoff of 2 units to determine significantly better support. When the  
<sup>207</sup> best fitting model was not significantly better than a less complex alternative, we selected  
<sup>208</sup> the least complex model (Appendix 12). We calculated model adequacy scores using the  
<sup>209</sup> R package *arbutus* (Pennell et al. 2015) (Appendix 13). We calculated phylogenetic signal  
<sup>210</sup> in each of the measured characters using Blomberg's K (Blomberg et al. 2003) (Appendix  
<sup>211</sup> 12), and for the morphological dataset as a whole using the R package *geomorph* (Adams et  
<sup>212</sup> al. 2016). We reconstructed ancestral states using Maximum Likelihood (`anc.ML` (Revell  
<sup>213</sup> 2012)), and stochastic character mapping (`make.simmap`) for categorical characters. R scripts  
<sup>214</sup> available in Dryad.

<sup>215</sup> In order to study the evolution of predatory specialization, we reconstructed components  
<sup>216</sup> of the diet and prey selectivity on the phylogeny using ML (R `phytools::anc.ML`). To identify  
<sup>217</sup> evolutionary associations of diet with tentillum and nematocyst characters, we compared the  
<sup>218</sup> performance of a neutral evolution model to that of a diet-driven directional selection model.  
<sup>219</sup> First, we collapsed the diet data into the five feeding guilds mentioned above (fish specialist,  
<sup>220</sup> small crustacean specialist, large crustacean specialist, gelatinous specialist, generalist), based

on which prey types they were observed consuming most frequently. We reconstructed the feeding guild ancestral states using the ML function `ace` (package `ape` (Paradis et al. 2019)), removing tips with no feeding data. The ML reconstruction was congruent with the consensus stochastic character mapping (Appendix 18). Then, using the package `OUwie` (Beaulieu and O'Meara 2012), we fitted an OU model with multiple optima and rates of evolution matched to the reconstructed ancestral diet regimes, a single optimum OU model, and a BM null model, inspired by the analyses in (Cressler et al. 2015). Finally, we compared their AICc support values to select the best fitting model (Appendix 14).

To model the evolutionary associations between individual tentillum and nematocyst characters and the ability to capture particular prey types in the diet, we ran a series of phylogenetic generalized linear models (R `phyloglm`) (Appendix 17). In addition, we ran a series of comparative analyses to address hypotheses of diet-tentillum relationships posed in the literature. To test for correlated evolution among binary characters, we used Pagel's test (Pagel 1994). To characterize and evaluate the relationship between continuous characters, we used phylogenetic generalized least squares regressions (PGLS) (Grafen 1989). To compare the evolution of continuous characters with categorical aspects of the diet, we carried out a phylogenetic logistic regression (R `nlme`):`gls`.

To generate hypotheses about the diets of understudied siphonophores for which no feeding observations have yet been reported (but for which we have tentacle morphology data), we carried out linear discriminant analysis of principal components (DAPC) using the `dapc` function (R `adegenet`):`dapc` (Jombart et al. 2010). This function allowed us to incorporate more predictors than individuals. We generated discriminant functions for feeding guild, soft/hard bodied prey, presence of copepods, fish, and shrimp (large crustaceans) in the diet (Appendix 15). Some taxa have inapplicable states for certain absent characters (such as the length of a nematocyst subtype that is not present in a species), which are problematic for DAPC analyses. We tackled this by transforming the absent states to zeroes. This approach allows us to incorporate all the data, but creates an attraction bias between

248 small character states (*e.g.* small tentilla) and absent states (*e.g.* no tentilla). Absent  
249 characters are likely to be very biologically relevant to prey capture and we believe they  
250 should be accounted for. We limited the number of linear discriminant functions retained  
251 to the number of groupings in each case. We selected the number of principal components  
252 retained using the a-score optimization function (R adegenet::optim.a.score) (Jombart et  
253 al. 2010) with 100 iterations, which yielded more stable results than the cross validation  
254 function (R adegenet::xval). This optimization aims to find the compromise value with highest  
255 discrimination power with the least overfitting. From these DAPCs we obtained the highest  
256 contributing morphological characters to the discriminaton (characters in the top quartile of  
257 the weighted sum of the linear discriminant loadings controlling for the eigenvalue of each  
258 discriminant). For each DAPC we generated hypotheses about the diets of siphonophores  
259 outside the training set (R adegenet::predict.dapc), incorporating prediction uncertainty as  
260 posterior probabilities (Appendix 15). In order to identify the sign of the relationship between  
261 the predictor characters prey type presence in the diet, we then generated generalized logistic  
262 regression models (as a type of generalized linear model, or GLM using R stats::glm) with the  
263 top contributing characters (from the corresponding DAPC) as predictors. We also carried  
264 out these GLMs on the Ivlev's selectivity indices for each prey type calculated from (Purcell  
265 1981) (in Appendix 11).

266 In order to explore the correlational structure among continuous characters and among  
267 their evolutionary histories, we used principal component analysis (PCA) and phylogenetic  
268 PCA (Revell 2012). Since the character data contains many gaps due to missing characters  
269 and inapplicable states, we carried out these analyses on a subset of species and characters  
270 that allowed for the most complete dataset. This was done by removing the terminal filament  
271 characters (which are only shared by a small subset of species), and then removing species  
272 which had inapplicable states for the remaining characters. In addition, we obtained the  
273 correlations between the phylogenetic independent contrasts (Felsenstein 1985) using the  
274 package rphylip (Revell and Chamberlain 2014).

275 To test how many times extreme nematocyst morphologies evolved, we reconstructed the  
276 ancestral states of  $\log(\text{length}/\text{width})$  of the different nematocyst types, and identified the  
277 branches with the greatest shifts. In addition to characterizing the shifts in the state values  
278 of haploneme and heteroneme elongation, we identified and located regime shifts for the rate  
279 of evolution using a Bayesian Analysis of Macroevolutionary Mixtures (BAMM) (Rabosky et  
280 al. 2014) (Appendix 16).

## 281 Results

282 *Phylogeny* – Only 5 nodes in the unconstrained inference were incongruent with the (Munro  
283 et al. 2018) transcriptome tree. The topology of the constrained tree presented here (Fig. 4)  
284 is congruent with the resolved nodes in (Dunn et al. 2005) and (Munro et al. 2018).

285 We retained the clade nomenclature defined in (Dunn et al. 2005) and (Munro et al.  
286 2018), such as Codonophora to indicate the sister group to Cystonectae, Euphysonectae to  
287 indicate the sister group to Calycophorae, Clade A and B to indicate the two main lineages  
288 within Euphysonectae. In addition, we define two new clades within Codonophora (Fig. 4):  
289 Eucladophora as the clade containing *Agalma elegans* and all taxa that are more closely related  
290 to it than to *Apolemia lanosa*, and Tendiculophora as the clade containing *Agalma elegans* and  
291 all taxa more closely related to it than to *Bargmannia elongata*. Eucladophora is characterized  
292 by bearing spatially differentiated tentilla with proximal heteronemes and a narrower terminal  
293 filament region. The etymology derives from the Greek *eu+kládos+phóros* for “true branch  
294 bearers”. Tendiculophora are characterized by bearing rhopalonemes and desmonemes in the  
295 terminal filament, having a pair of elastic strands, and developing proximally detachable  
296 cnidobands. The etymology of this clade is derived from the Latin *tendicula* for “snare or  
297 noose” and the Greek *phóros* for “carriers”.

298 *Evolutionary dynamics between diet and tentillum morphology* – The reconstructions of  
299 feeding guilds show that generalism is not likely to be ancestral, and it appears to have evolved  
300 at least two times independently (Fig. 5). Generalism evolves twice independently from

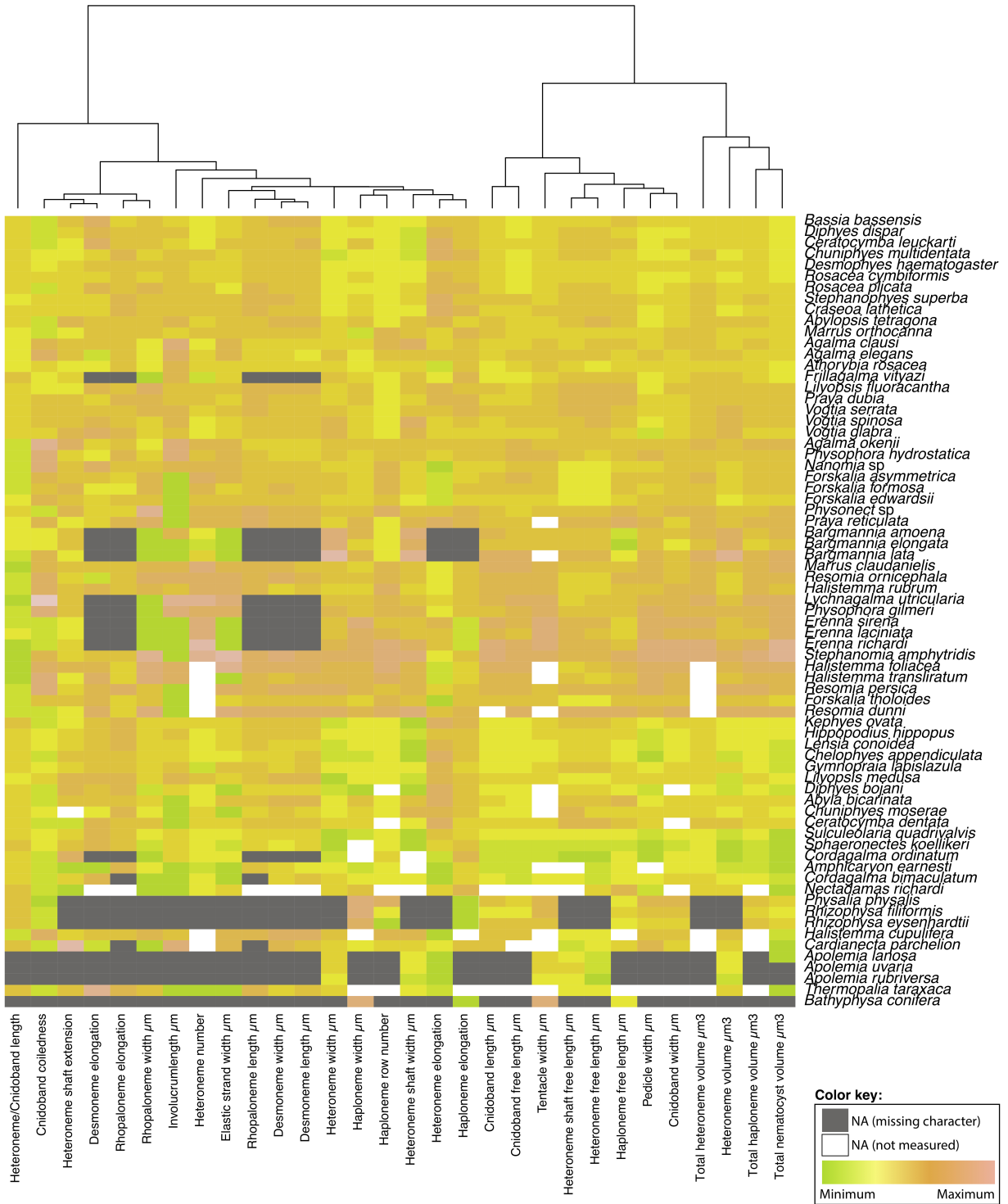


Figure 3: Heatmap summarizing the morphological diversity measured for 96 species of siphonophores clustered by similarity (raw data in Appendix 3). Missing values from absent characters presented as dark grey cells, missing values produced from technical difficulties presented as white cells. Values scaled by character.

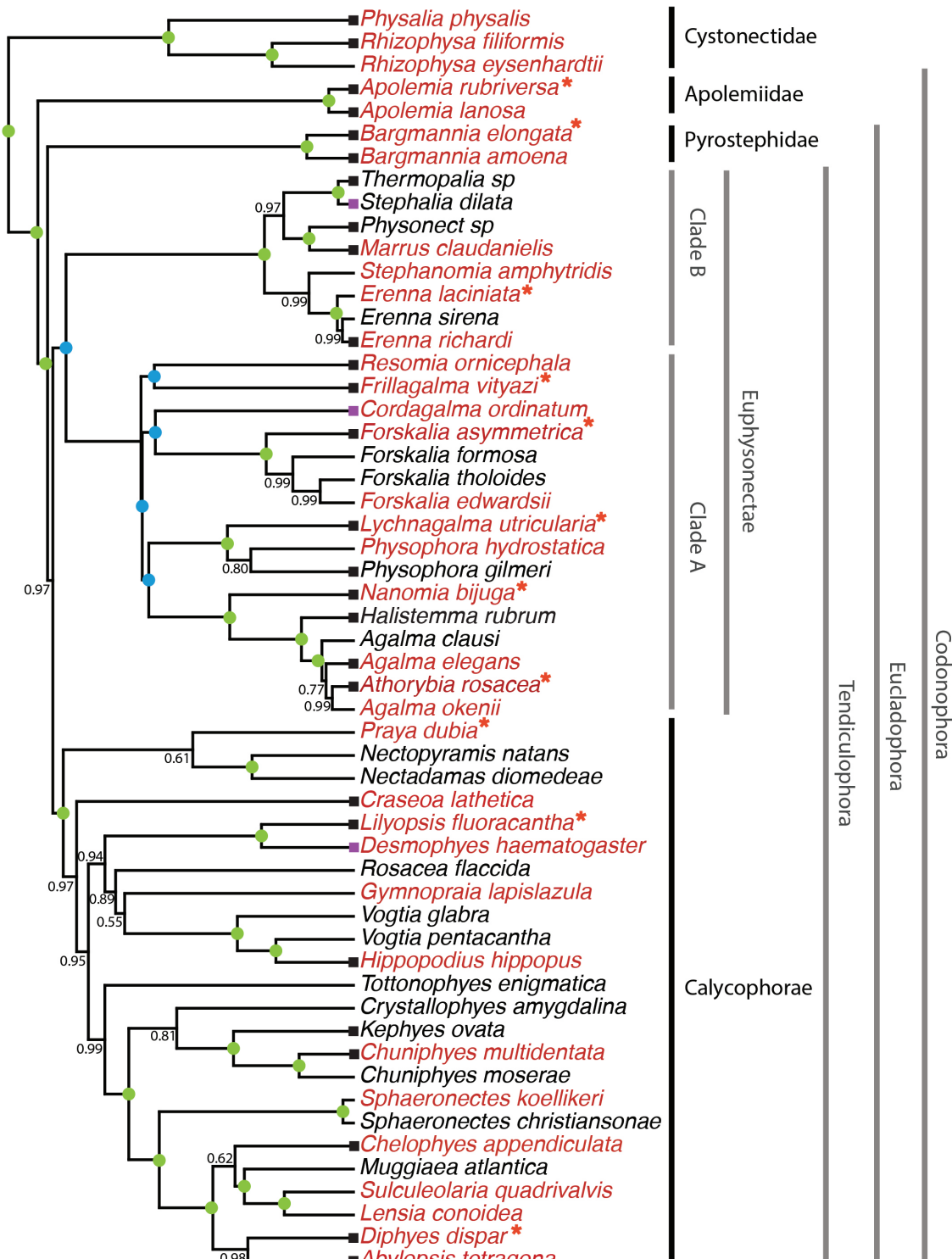


Figure 4: Bayesian time-tree built from 18S + 16S concatenated sequences. Branch lengths estimated using relaxed molecular clock. Species names in red indicate replicated representation in the morphology data. Species marked with an asterisk were recorded using high speed video. Nodes labeled with bayesian posteriors (BP). Green circles indicate BP = 1. Blue circles indicate nodes constrained to be congruent with (Munro *et al.* 2018). Tips with black squares indicate the species with transcriptomes used in (Munro *et al.* 2018). Tips with grey squares indicate genus-level correspondence to taxa included in (Munro *et al.* 2018). The tree includes 150 taxa, 150 tips, 150 nodes, 150 branch lengths, and 150 posterior probabilities.

301 large crustacean specialist lineages, supporting hypothesis 3. Feeding guild specializations  
302 have shifted from an alternative ancestral state at least five times, supporting hypothesis  
303 2. Individual prey type presence reconstructions show that copepod specialization and fish  
304 specialization evolved twice, ostracod specialization evolved at least once. The OUwie model  
305 comparison shows that out of 30 characters, 10 show significantly stronger support for the  
306 diet-driven multi-optima multi-rate OU model (Appendix 14). These characters include  
307 terminal filament nematocyst size and shape, involucrum length, elastic strand width, and  
308 heteroneme number. Most of these characters are found exclusively in Tendiculophora,  
309 thus this reflects processes that could be unique to this subtree. Five characters including  
310 cnidoband length, cnidoband shape, and haploneme length show maximal support for a  
311 diet-driven single-optimum OU model. The remaining 15 characters support BM (or OU  
312 with marginal AICc difference with BM).

313 Phylogenetic logistic regressions identified evolutionary associations between individual  
314 characters and the presence of particular prey types in the diet (Fig. 5, right). Shifts toward  
315 ostracod presence in diet correlated with reductions in pedicle width and total haploneme  
316 volume. Shifts to copepod presence in the diet were associated with reductions in haploneme  
317 width, cnidoband length and width, total haploneme and heteroneme volumes, and tentacle  
318 and pedicle widths. Consistently, transitions to decapod presence in the diet correlated with  
319 more coiled cnidobands (Appendix 17).

320 Phylogenetic regressions of continuous characters against prey selectivity data produced  
321 additional insights. Fish selectivity is associated with increased number of heteronemes  
322 per tentillum, increased roundness of nematocysts (desmonemes and haplonemes), larger  
323 heteronemes, reduced heteroneme/cnidoband length ratios, smaller rhopalonemes, lower  
324 haploneme SA/V ratios, and increased size of the cnidoband, elastic strand, pedicle and  
325 tentacle widths. Decapod-selective diets were associated with increasing cnidoband size and  
326 coiledness, haploneme row number, elastic strand width, and heteroneme number. Copepod-  
327 selective diets evolved in association with smaller heteroneme and total nematocyst volumes,

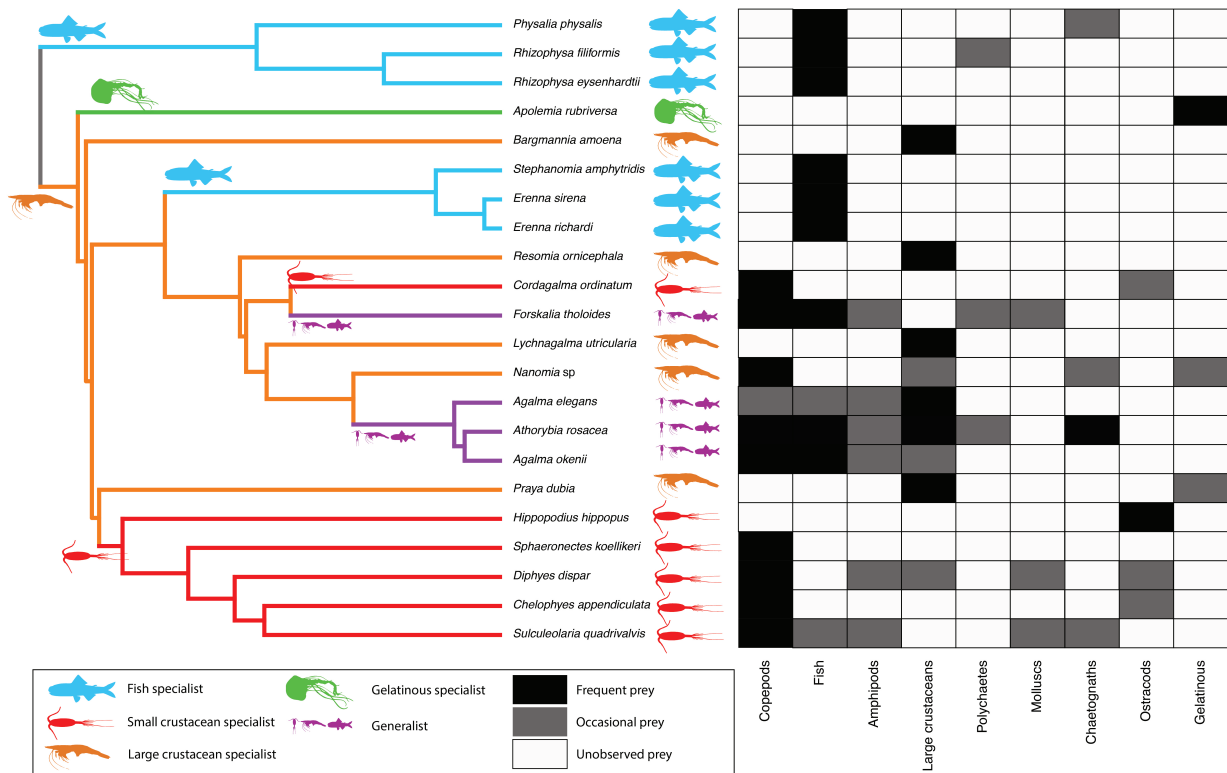


Figure 5: Left - Subset phylogeny showing the mapped feeding guild regimes that were used to inform the *OUwie* analyses. Right - Grid showing the prey items consumed from which the feeding guild categories were derived. Diet data were obtained from the literature review in Appendix 10.

328 smaller cnidobands, rounder rhopalonemes, elongated heteronemes, narrower haplonemes  
329 with higher SA/V ratios, and smaller heteronemes, tentacles, pedicles and elastic strands.  
330 Selectivity for ostracods was associated with reductions in size and number of heteroneme  
331 nematocysts, reductions in cnidoband size, number of haploneme rows, heteroneme number,  
332 and cnidoband coiledness. Heteroneme length and shape also correlated negatively with  
333 chaetognath selectivity.

334 When some of the diet-morphology associations reported in the literature (Purcell 1984;  
335 Purcell and Mills 1988) were tested for correlated evolution (Table 1), we found that most  
336 were consistent with an evolutionary explanation except the relationship between terminal  
337 filament nematocysts (rhopalonemes and desmonemes) and crustaceans in the diet. The latter  
338 is likely a product of the larger species richness of crustacean-eating species with terminal  
339 filament nematocysts, rather than simultaneous evolutionary gains.

340 Table 1. Tests of correlated evolution between morphological characters and aspects of  
341 the diet found correlated in the literature.

Character	Aspect of diet	Test of evolutionary association	Relationship sign	P-value	Number of taxa	Association first report
Differentiated cnidobands	Hard bodied prey	Page's test	+	0.017	19	Purcell, 1984
Heteroneme volume	Copepod prey size	pGLS	+	0.002	8	Purcell, 1984
Terminal filament nematocysts	Crustacean diet	Page's test	+	0.200	19	Purcell & Mills, 1988
Number of nematocyst types	Soft-bodied prey	Phylogenetic logistic regression	-	0.040	22	Purcell & Mills, 1988

342

343

344 *Generating dietary hypotheses using tentillum morphology* – The discriminant analysis of  
345 principal components for feeding guild (7 principal components, 4 discriminants) produced  
346 100% discrimination, and the highest loading contributions were found for the characters  
347 (ordered from highest to lowest): Involucrum length, heteroneme volume, heteroneme number,  
348 total heteroneme volume, tentacle width, heteroneme length, total nematocyst volume, and  
349 heteroneme width (Appendix 15.1). We used the predictions from this discriminant function  
350 to generate hypotheses about the feeding guild of 45 species in our morphological data (Fig.  
351 @((figure6))). This projection predicts that two other *Apolemia* species may also be gelatinous  
352 prey specialists like *Apolemia rubriversa*, and that *Erenna laciniata* may be a fish specialist

353 like *Erenna richardi*.

354 Table 2. Discriminant analysis of principal components for the presence of specific prey  
355 types using the morphological data. Top quartile variable (character) contributions to the  
356 linear discriminants are ordered from highest to lowest. Logistic regressions and GLMs were  
357 fitted to predict prey type presence and selectivity respectively. The sign of the slope of each  
358 predictor is reported, and highlighted green if significant ( $p$  value  $< 0.05$ ). Pseudo- $R^2$  (%)  
359 approximates the percent variance explained by the model.

Prey type	DAPC	GLM for prey type presence (22 taxa)		Best fitting GLM for prey type selectivity (Purcell, 1981) (7 taxa)	
		Discrimination (%)	Top quartile variable contributions	Sign	Pseudo- $R^2$ (%)
Copepods	95.4	Total nematocyst volume	-	-	
		Tentacle width	-	+	
		Haploneme elongation	-	+	
		Haploneme surface area/volume ratio	+	-	
		Haploneme row number	+	+	
		Cnidoband length	-	+	
		Cnidoband width	-	-	
		Cnidoband free length	+	+	
Fish	68.1	Total haploneme volume	-	+	
		Heteroneme volume	+	-	
		Total nematocyst volume	-	+	
		Total heteroneme volume	-	-	
		Cnidoband length	-	-	
		Cnidoband free length	+	+	
		Involucrum length	-	-	
		Pedicle width	+	+	
Large crustaceans	81.8	Involucrum length	+	+	
		Total heteroneme volume	-	-	
		Elastic strand width	-	+	
		Rhopaloneme length	+	+	
		Heteroneme volume	+	-	
		Haploneme elongation	-	+	
		Desmoneme length	-	-	
		Tentacle width	+	+	

360

361 When predicting soft and hard bodied prey specialization, the DAPC achieved 90.9%  
362 discrimination success, only marginally confounding hard-bodied specialists with generalists  
363 (Appendix 15.4). The main characters driving the discrimination are involucrum length,  
364 heteroneme number, heteroneme volume, tentacle width, total nematocyst volume, total  
365 haploneme volume, elastic strand width, and heteroneme length. Discriminant analyses and  
366 GLM logistic regressions were also applied to specific prey type presence and selectivity  
367 (Table 2), revealing the sign of their predictive relationship to each prey type. We only  
368 selected prey types with sufficient variation in the data to carry out these analyses (copepods,  
369 fish, and large crustaceans). While the presence of fish or large crustaceans in the diet cannot  
370 be unambiguously discriminated using tentillum morphology (Appendix 15), specialization

<sup>371</sup> on fish or large crustacean prey can be fully disentangled (Appendix 15.1). For each prey  
<sup>372</sup> type studied, tentilla morphology is a much better predictor of prey selectivity than of  
<sup>373</sup> prey presence, despite prey selectivity data being available for a smaller subset of species.  
<sup>374</sup> Interestingly, many of the morphological predictors had opposite slope signs when predicting  
<sup>375</sup> prey selectivity *versus* predicting prey presence in the diet (Table 2).

<sup>376</sup> *Evolution of tentillum and nematocyst characters* – One third of the characters measured  
<sup>377</sup> support a non-phylogenetic generative model, indicating they are not likely to be phylogeneti-  
<sup>378</sup> cally distributed (Appendix 12). Total nematocyst volume and cnidoband-to-heteroneme  
<sup>379</sup> length ratio showed strongly conserved phylogenetic signals. 74% of characters present a  
<sup>380</sup> significant phylogenetic signal, yet only total nematocyst volume, haploneme length, and  
<sup>381</sup> heteroneme-to-cnidoband length ratio had a phylogenetic signal  $K > 1$ . 67% of characters  
<sup>382</sup> support BM models, indicating a history of neutral constant divergence. No relationship  
<sup>383</sup> between phylogenetic signal and BM model support was found. Haploneme nematocyst  
<sup>384</sup> length is the only character with support for an EB model of decreasing rate of evolution  
<sup>385</sup> with time. No character had support for a single-optimum OU model (when uninformed by  
<sup>386</sup> feeding guild regime priors).

<sup>387</sup> The phylogenetic positions of the main categorical character shifts were reconstructed  
<sup>388</sup> using stochastic character mappings (Appendix 18), and summarized in Figure 7. Haploneme  
<sup>389</sup> nematocysts are likely ancestrally present in the tentacles, since they are present in the  
<sup>390</sup> tentacles of many other hydrozoans. Haplonemes diverged into spherical isorhizas of 2  
<sup>391</sup> size classes in Cystonectae, and elongated anisorhizas of one size class in Codonophora.  
<sup>392</sup> Haplonemes were likely lost in the tentacles of *Apolemia*, but spherical isorhizas are retained  
<sup>393</sup> in other *Apolemia* tissues (Siebert et al. 2013). Similarly, while heteronemes exist in other  
<sup>394</sup> tissues of cystonects, they only appear in the tentacles of codonophorans as birhopaloids in  
<sup>395</sup> *Apolemia*, ancestral stenoteles in eucladophoran physonects, and microbasic mastigophores in  
<sup>396</sup> calycophorans.

<sup>397</sup> Eucladophora (the clade containing Pyrostephidae, Euphysonectae, and Calycophorae,

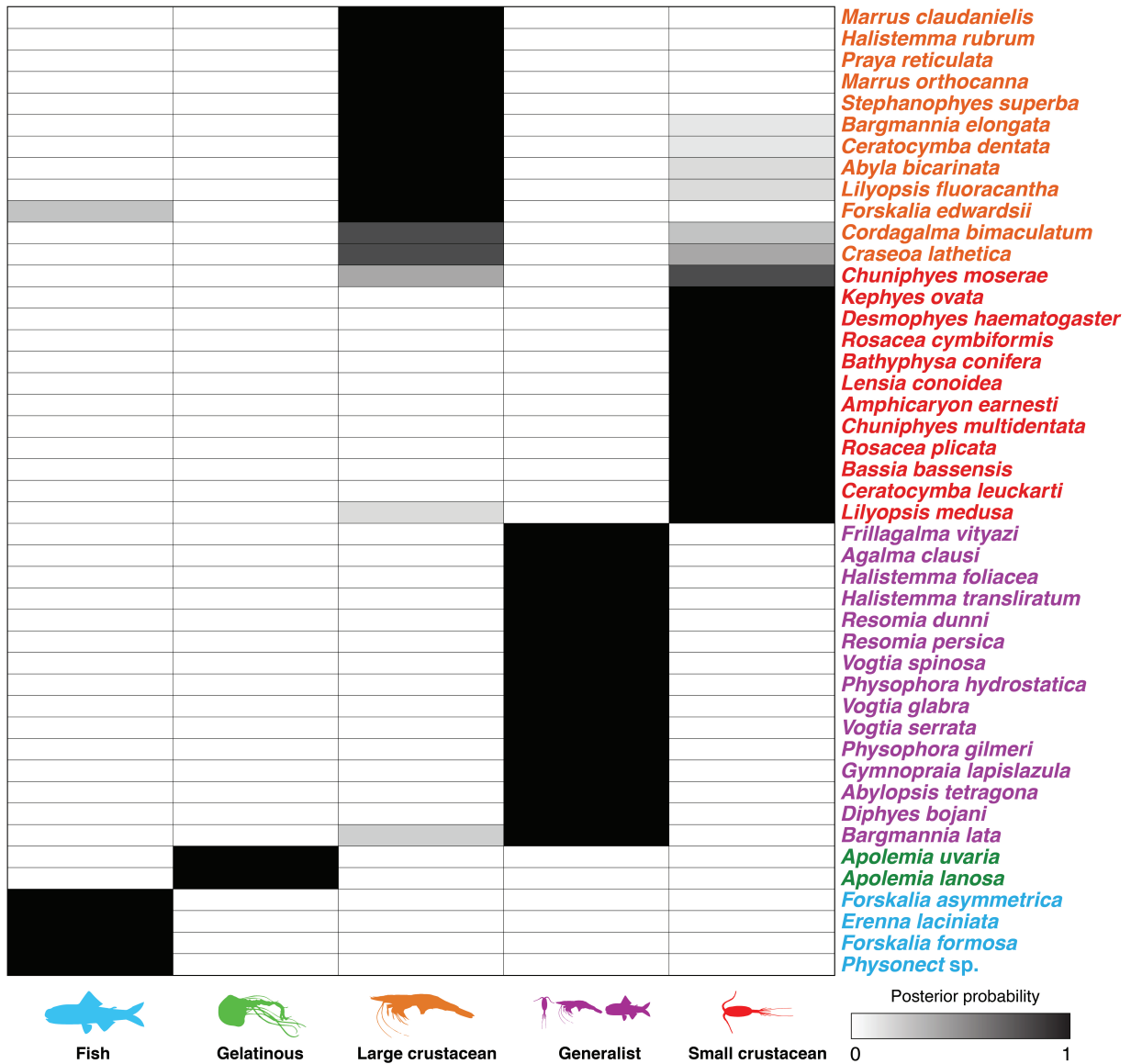


Figure 6: Hypothetical feeding guilds for siphonophore species predicted by a 6 PCA DAPC (in Appendix 15.1). Cell darkness indicates posterior probability of belonging to each guild. Training data set transformed so inapplicable states are computed as zeroes. Species ordered and colored according to their predicted feeding guild.

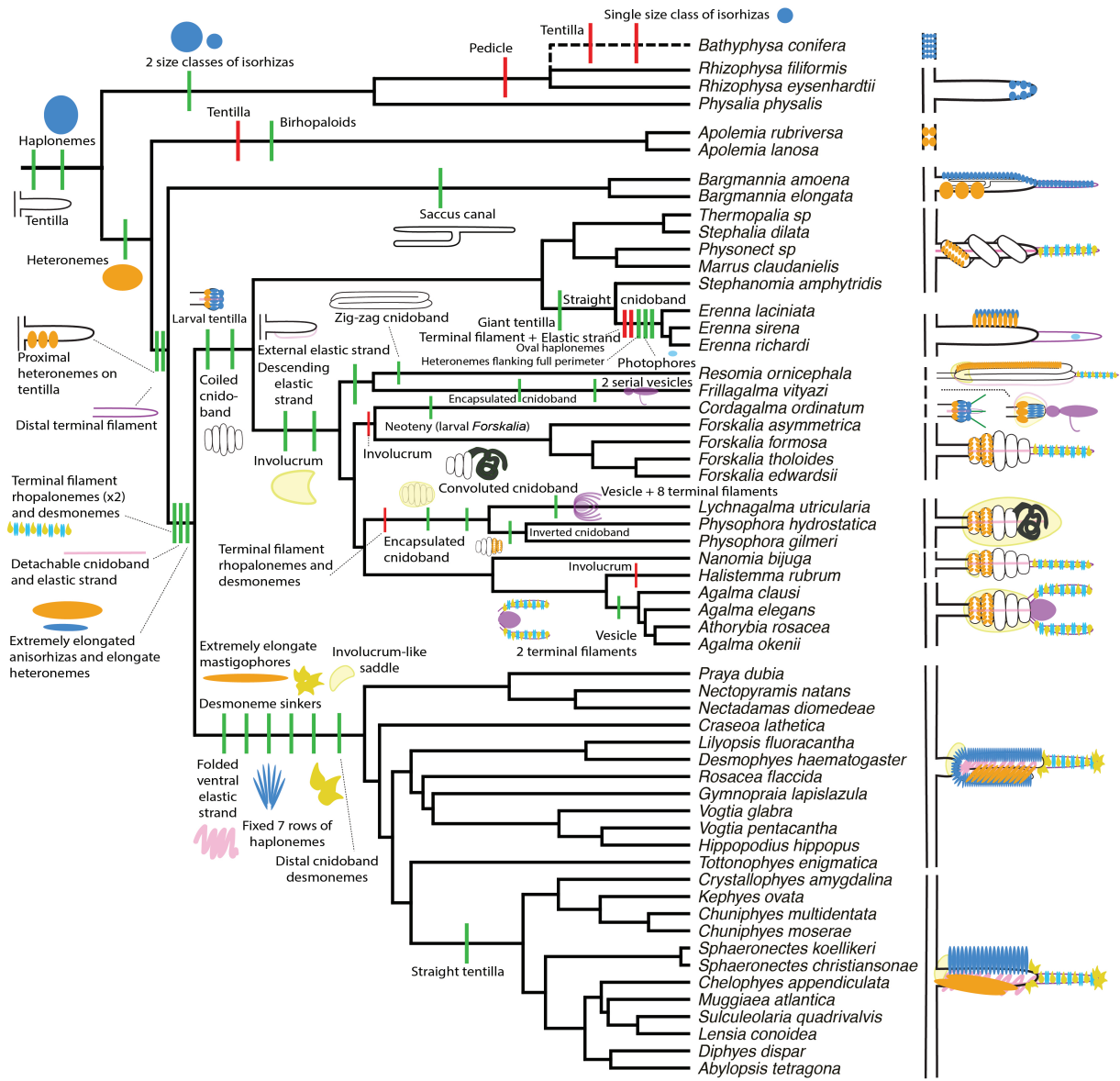


Figure 7: Siphonophore cladogram with the main categorical character gains (green) and losses (red) mapped. Some branch lengths were modified from the Bayesian chronogram to improve readability. The main visually distinguishable tentillum types are sketched next to the species that bear them, showing the location and arrangement of the main characters. In large complex-shaped tentilla, haplonemes were omitted for simplification. The rhizophysid *Bathyphysa conifera* branch was appended manually as a polytomy (dashed line).

398 see Fig. 4) encompasses most of the extant Siphonophore species (178 of 186). Innovations  
399 evolved in the stem of this group include spatially segregated heteroneme and haploneme  
400 nematocysts, terminal filaments, and elastic strands (Fig. 7). Pyrostephids evolved a unique  
401 bifurcation of the axial gastrovascular canal of the tentillum known as the “saccus” (Totton  
402 and Bargmann 1965). The stem to the clade Tendiculophora (clade containing Euphysonectae  
403 and Calycophorae, see Fig. 4) subsequently acquired further novelties such as the desmoneme  
404 and rhopaloneme (acrophore subtype ancestral) nematocysts on the terminal filament (Fig.  
405 7), which bear no other nematocyst type (Fig. 1). These are arranged in sets of 2 parallel  
406 rhopalonemes for each single desmoneme (Skaer 1988, 1991). The involucrum is an expansion  
407 of the epidermal layer that can cover part or all of the cnidoband (Fig. 2). This structure,  
408 together with differentiated larval tentilla, appeared in the stem branch to Clade A physonects.  
409 Calycophorans evolved unique novelties such as larger desmonemes at the distal end of the  
410 cnidoband, pleated pedicles with a “hood” (here considered homologous to the involucrum) at  
411 the proximal end of the tentillum, anacrophore rhopalonemes, and microbasic mastigophore-  
412 type heteronemes. While calycophorans have diversified into most of the extant described  
413 siphonophore species (108 of 186), their tentilla have not undergone any major categorical  
414 gains or losses since their most recent common ancestor. Nonetheless, they have spreaded  
415 over a broad span of variation in nematocyst and cnidoband sizes.

416       *Phenotypic integration of the tentillum* – The quantitative characters we measured from  
417 tentilla and their nematocysts are highly correlated. The results indicate that the dimen-  
418 sionality of tentillum morphology is low, that many traits are associated with size, but that  
419 nematocyst arrangement and shape are independent of it. Of the phylogenetic correlations  
420 (Fig. 8a, lower triangle), 81.3% were positive and 18.7% were negative, while of the ordinary  
421 correlations (Fig. 8a, upper triangle) 74.6% were positive and 25.4% were negative. Half  
422 (49.9%) of phylogenetic correlations were  $>0.5$ , while only 3.6% are  $< -0.5$ . Similarly, of  
423 the across-species correlations, 49.1% were  $>0.5$  and only 1.5% were  $< -0.5$ . 13.9% of char-  
424 acter pairs had opposing phylogenetic and ordinary correlation coefficients. Just 4% have

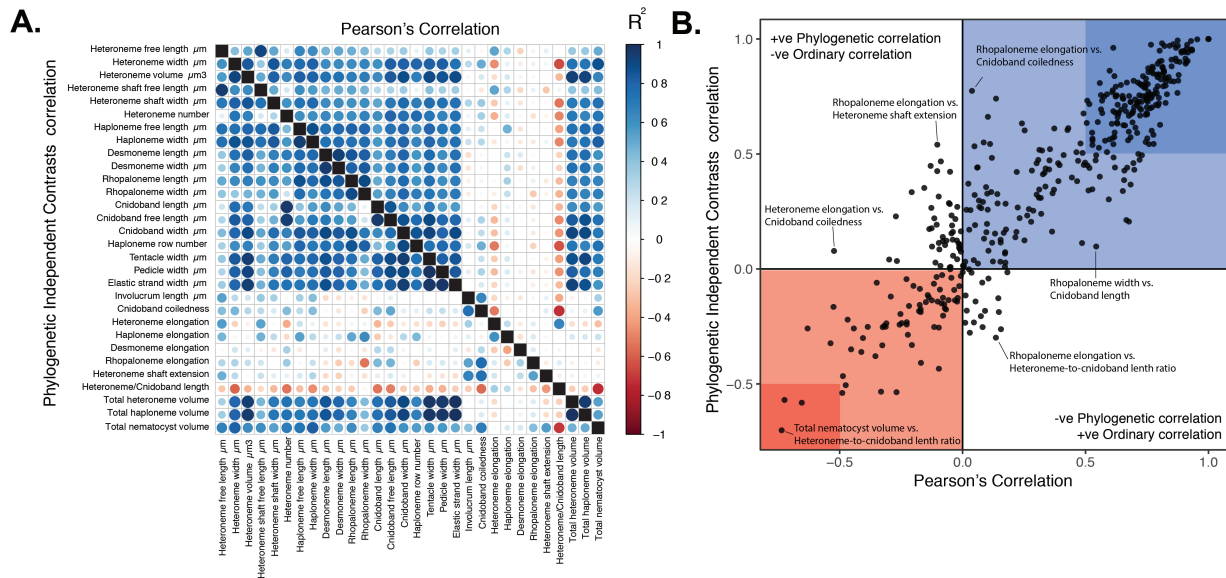


Figure 8: A. Correlogram showing strength of ordinary (upper triangle) and phylogenetic (lower triangle) correlations between characters. Both size and color of the circles indicate the strength of the correlation ( $R^2$ ). B. Scatterplot of phylogenetic correlation against ordinary correlation showing a strong linear relationship ( $R^2 = 0.92$ , 95% confidence between 0.90 and 0.93). Light red and blue boxes indicate congruent negative and positive correlations respectively. Darker red and blue boxes indicate strong ( $<-0.5$  or  $>0.5$ ) negative and positive correlation coefficients respectively.

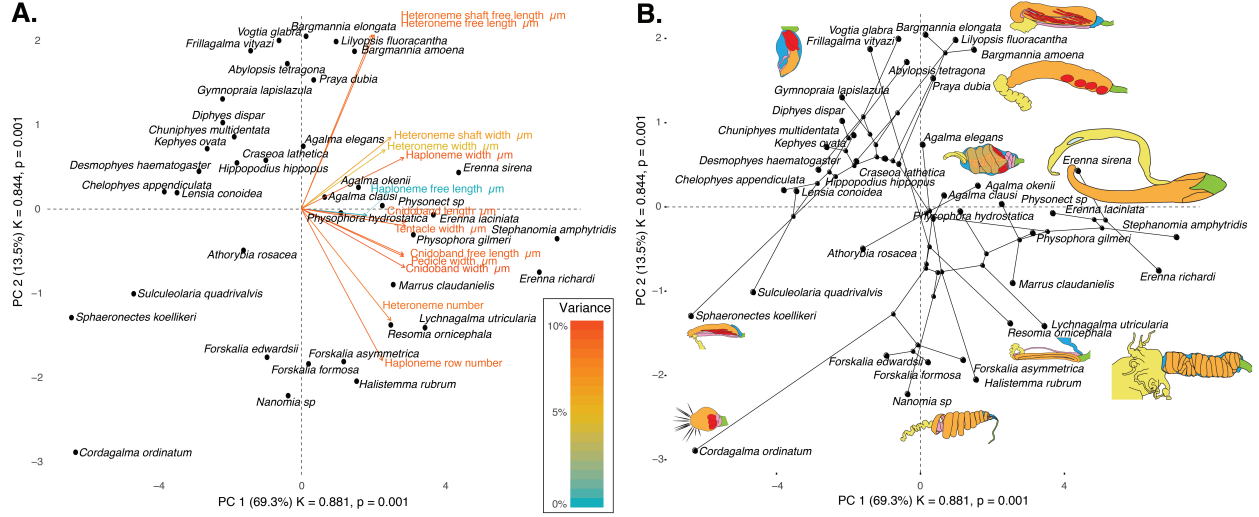


Figure 9: Phylomorphospace of the simple continuous characters principal components, excluding ratios and composite characters. A. Variance explained by each variable in the PC1-PC2 plane. Axis labels include the phylogenetic signal (K) for each component and p-value. B. Phylogenetic relationships between the species points distributed in that same space.

negative phylogenetic and positive ordinary correlations (such as rhopaloneme elongation ~ heteroneme-to-cnidoband length ratio and haploneme elongation, or haploneme elongation ~ heteroneme number), and vice versa for 9.9% of character pairs (such as heteroneme elongation ~ cnidoband convolution and involucrum length, or rhopaloneme elongation with cnidoband length). These disparities can be caused by Simpson's paradox (Blyth 1972), the reversal of the sign of a relationship when a third variable (or a phylogenetic topology (Uyeda et al. 2018)) is considered. However, no character pair had correlation coefficient differences larger than 0.64 between ordinary and phylogenetic correlations (heteroneme shaft extension ~ rhopaloneme elongation has a Pearson's correlation of 0.10 and a phylogenetic correlation of -0.54). Rhopaloneme shape shows the most incongruences between phylogenetic and ordinary correlations with other characters.

In the non-phylogenetic PCA morphospace using only simple characters (Fig. 9), PC1 (aligned with tentillum and tentacle size) explained 69.3% of the variation in the tentillum morphospace, whereas PC2 (aligned with heteroneme length, heteroneme number, and haploneme arrangement) explained 13.5%. In a phylogenetic PCA, 63% of the evolutionary

<sup>440</sup> variation in the morphospace is explained by PC1 (aligned with shifts in tentillum size), while  
<sup>441</sup> 18% is explained by PC2 (aligned with shifts in heteroneme number and involucrum length).

<sup>442</sup>        *Evolution of nematocyst shape* – Haploneme nematocyst evolution has been mainly  
<sup>443</sup> driven by a single large shift towards elongation in Tendiculophora, which contains the  
<sup>444</sup> majority of described siphonophore species. There is one secondary return to more oval, less  
<sup>445</sup> elongated haplonemes in *Erenna*, but it doesn't reach the sphericity present in Cystonectae  
<sup>446</sup> or Pyrostephidae (Fig. 10). Heteroneme evolution presents a less radical evolutionary history,  
<sup>447</sup> where Tendiculophora evolved more elongate heteronemes, but the difference between theirs  
<sup>448</sup> and other siphonophores is much smaller than the variation in shape within Tendiculophora,  
<sup>449</sup> bearing no phylogenetic signal. In this group, the evolution of heteroneme shape has diverged  
<sup>450</sup> in both directions, and there is no correlation with haploneme shape, which has remained  
<sup>451</sup> fairly constant (elongation between 1.5 and 2.5).

<sup>452</sup>        Haploneme and heteroneme shape share 21% of their variance across extant values, and  
<sup>453</sup> 53% of variance in their shifts along the branches of the phylogeny. However, much of this  
<sup>454</sup> correlation is due to the contrast between Pyrostephidae and their sister group Tendiculophora  
<sup>455</sup> (Fig. 4). BAMM identified a regime shift in heteroneme shape evolution on the branches  
<sup>456</sup> leading to *Agalma* and *Athorybia*. For the rates of haploneme shape evolution, BAMM  
<sup>457</sup> identified two main independent regime shifts (Fig. 10): one in the branch leading to  
<sup>458</sup> Codonophora (anisorhizas diverging from cystonects' spherical isorhizas), and one in the  
<sup>459</sup> branch leading to Clade B physonects. Clade B includes *Erenna*, *Stephanomia*, *Marrus*, and  
<sup>460</sup> rhodaliids. Most of these taxa have rod-shaped anisorhizas, but *Erenna* has oval ones). No  
<sup>461</sup> clear regime shift patterns were identified in the evolution of desmoneme and rhopaloneme  
<sup>462</sup> shape.

<sup>463</sup>        *Functional morphology of tentillum and nematocyst discharge* – Tentillum and nematocyst  
<sup>464</sup> discharge high speed measurements are available in Appendix 4. While the sample sizes of  
<sup>465</sup> these measurements were insufficient to draw reliable statistical results at a phylogenetic level,  
<sup>466</sup> we did observe patterns that may be relevant to their functional morphology. For example,

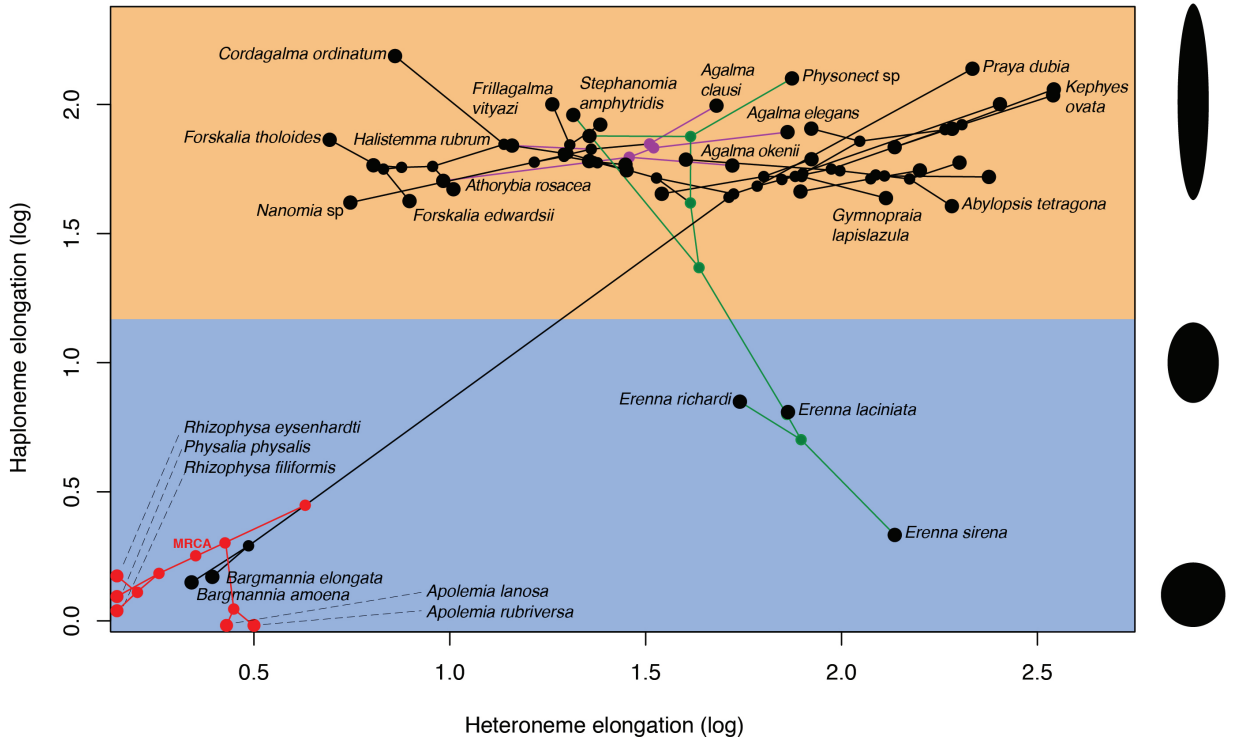


Figure 10: Phylomorphospace showing haploneme and heteroneme elongation (log scaled). Orange area delimits rod-shaped haplonemes, blue area covers oval and round shaped haplonemes. Smaller dots and lines represent phylogenetic relationships and ancestral states of internal nodes under BM. Species nodes in red were manually added to the plot. Cystonects have no tentacle heteronemes and are projected onto the haploneme axis. Apolemids have no tentacle haplonemes and are projected onto the heteroneme axis. Colored branches and nodes correspond to BAMM regimes of accelerated haploneme shape (green) and heteroneme shape (violet) evolution.

467 cnidoband length is strongly correlated with discharge speed (p value = 0.0002). This is  
468 probably the sole driver of the considerable difference between euphysonect and calycophoran  
469 tentilla discharge speeds (average discharge speeds: 225.0mm/s and 41.8mm/s respectively;  
470 t-test p value = 0.011), since the euphysonects have larger tentilla than the calycophorans  
471 among the species recorded.

472 We also observed that calycophoran haploneme tubules fire faster than those of eu-  
473 physonects (T-test p value = 0.001). Haploneme nematocysts discharge 2.8x faster than  
474 heteroneme nematocysts (T-test p value = 0.0012). Finally, we observed that the stenoteles  
475 of the Euphysonectae discharge a helical filament that “drills” itself through the medium it  
476 penetrates as it everts.

## 477 Discussion

478 The core aims of this study are to examine the evolutionary history of siphonophore tentilla and  
479 diet, characterize the evolutionary shifts in their trophic niches, and identify the morphological  
480 characters that evolve with changes in prey type. We inquire whether the relationships between  
481 form and function observed in extant taxa are due to correlated evolution or non-evolutionary  
482 causes, whether the evolution of their trophic specializations supports or challenges traditional  
483 ecological theory (such as the idea specialists evolve from generalists), and whether the diets  
484 of siphonophores can be hypothesized by observing their tentacles. In addition, we produced  
485 novel findings on tentillum morphology, siphonophore phylogeny, nematocyst character  
486 evolution, and tentillum discharge dynamics.

487 *Evolution of tentillum morphology with diet* – Siphonophores are an abundant group of  
488 zooplankton in oceanic ecosystems (Longhurst 1985; O’Brien 2007). While little is known  
489 about siphonophore trophic ecology, what is known indicates that they occupy a central  
490 position in midwater food webs (Choy et al. 2017), serving as trophic intermediaries between  
491 smaller zooplankton and higher trophic level predators. Siphonophore species have been  
492 observed to feed on a variety of prey with very different sizes, traits, and behaviors. Because

493 there is a total absence of siphonophores in the fossil record, how they became established  
494 as the ubiquitous and diversified predators in today's oceans remains an open question.  
495 Predators that use similar tools for prey capture tend to capture similar prey, so their  
496 abundance and coexisting species diversity are inversely related due to competitive exclusion  
497 by resource limitation (Schluter 2000). However, this is not consistent with what we observe  
498 in siphonophores, which have been found to be both very abundant and locally diverse  
499 (Longhurst 1985, @mapstone2014global). We hypothesize that siphonophores have escaped  
500 this by specializing on different prey resources.

501 According to our reconstructions, the evolutionary history of siphonophore diets indicates  
502 that being a specialist was an ancestral aspect of their trophic niche, while trophic generalism  
503 is likely a derived condition. Several studies (reviewed in (Futuyma and Moreno 1988))  
504 have suggested that resource specialization is an irreversible dead end due to the constraints  
505 posed by phenotypic specialization. Our reconstructions show that this is not the case for  
506 siphonophores, where the prey type on which they specialize has shifted at least 5 times, and  
507 generalism has evolved independently at least twice. Among the evolutionary hypotheses  
508 considered, we find support for both hypotheses 2 (specialist resource switching) and 3  
509 (specialist to generalist), but no support for hypothesis 1 (generalist to specialist). The  
510 evolutionary history of tentilla shows that siphonophores are an example of trophic niche  
511 diversification via morphological innovation and evolution, which allowed transitions between  
512 specialized trophic niches. This strategy is particularly important in a deep open ocean  
513 ecosystem, which is a relatively homogeneous physical environment, where the primary niche  
514 heterogeneity available is the potential interactions between organisms (Robison 2004).

515 One of the most common prey items found in siphonophore diets is copepods (Fig. 5).  
516 Copepod-specialized diets have evolved convergently in *Cordagalma* and some Calycophorans.  
517 These evolutionary transitions happened together with transitions to smaller tentilla with  
518 fewer cnidoband nematocysts. Tentilla are expensive single-use structures, therefore we would  
519 expect that specialization in small prey would beget reductions in the size of the prey capture

520 apparatus to the minimum required for the ecological function. *Cordagalma*'s tentilla strongly  
521 resemble the larval tentilla (only found in the first-budded feeding body of the colony) of  
522 their sister genus *Forskalia* spp. This indicates that the evolution of *Cordagalma* tentilla  
523 could be a case of paedomorphosis associated with predatory specialization.

524 (Purcell 1984) showed that haplonemes have a penetrating function as isorhizas in  
525 cystonects and an adhesive function as anisorrhizas in Tendiculophora. The two clades that  
526 have been observed primarily feeding on fish (Cystonectae and Clade B, which includes  
527 *Erenna*, *Stephanomia*, *Marrus*, and rhodaliids) present an accelerated rate of haploneme  
528 shape evolution towards more compact haplonemes, significantly distinct from their closest  
529 relatives. Isorhizas in cystonects are known to penetrate the skin of fish during prey capture,  
530 and to deliver the toxins that aid in paralysis and digestion (Hessinger 1988). *Erenna*  
531 anisorrhizas are also able to penetrate human skin and deliver a painful sting (Pugh 2001)  
532 (and pers. obs.), a common feature of piscivorous cnidarians like cystonects or cubozoans.

533 (Thomason 1988) hypothesized that smaller, more spherical nematocysts, with a lower  
534 surface area to volume ratio, are more efficient in osmotic-driven discharge and thus have  
535 more power for skin penetration. The elongated haplonemes of crustacean-eating Tendicu-  
536 lophora have never been observed penetrating their crustacean prey ((Purcell 1984) and our  
537 unpublished observations), and are hypothesized to entangle the prey through adhesion of  
538 the abundant spines to the exoskeletal surfaces and appendages. Entangling requires less  
539 acceleration and power during discharge than penetration, as it does not rely on point pressure.  
540 In fish-eating cystonects and *Erenna* species, the haplonemes are much less elongated and  
541 very effective at penetration, in congruence with the osmotic discharge hypothesis. The  
542 accelerated rate of heteroneme shape diversification in the smallest clade containing *Agalma*  
543 and *Nanomia* may indicate a rapid dietary differentiation. However, our limited ecological  
544 data do not show any significant dietary differentiation in this group.

545 When we tested the diet-morphology correlation hypotheses supported in the literature  
546 from a macroevolutionary perspective, we found that most of them were consistent with

547 correlated evolution (Table 2). The ecomorphological association between rhopalonemes,  
548 desmonemes, and crustacean eaters was not congruent with a scenario of correlated evolution.  
549 This could be due to the broader set of taxa in our analyses, including multiple species  
550 without desmonemes or rhopalonemes but which effectively capture crustaceans (such as  
551 *Cordagalma ordinatum*, *Lychnagalma utricularia*, and *Bargmannia amoena*).

552 While our results unambiguously show that tentillum morphology evolved with diet, the  
553 conclusions we can draw from these analyses are limited by the sparse dietary data available.  
554 Moreover, our analyses are not sufficient to adequately test hypotheses of adaptation, since  
555 that would require evidence of changes within a population exposed to different selective  
556 pressures. When interpreting these results, it is important to remember that diet is a product  
557 of environmental prey availability and predator selectivity. Selectivity differences across  
558 siphonophore species could be driven by other phenotypes not accounted for this study. For  
559 example, tentacle-deploying behavior, positioning in the water column, or thresholds for  
560 discharging on or ingesting an encountered animal. Further observations on these behaviors in  
561 the field are necessary to assess their relative importance in determining dietary composition.  
562 In addition to behavior, there is much biochemistry in the prey capture and digestion processes  
563 that remains unexplored. Part of the success in siphonophore prey capture is likely determined  
564 by the effectiveness of the toxins delivered by the nematocysts on different taxa. Comparative  
565 toxin assays and venom protein evolution studies could shed light on this question. Moreover,  
566 siphonophore trophic specialization may have brought changes in the digestive biochemistry  
567 of gastrozooids and palpons. A comparison of the gene expression levels for different enzymes  
568 in the gastrozooids of different species, together with digestive enzyme sequence evolution  
569 studies, and a toxicological assay of the different venoms in siphonophore nematocysts on  
570 different prey taxa, would provide a great complement to our results.

571 *Generating hypotheses on siphonophore feeding ecology* – One motivation for our research  
572 was to understand the links between predator capture tools and their diets so we can generate  
573 hypotheses about the diets of siphonophores based on morphological characteristics. Indeed,

574 our discriminant analyses were able to distinguish between different siphonophore diets  
575 based on morphological characters alone. The models produced by these analyses generated  
576 testable predictions about the diets of many species for which we only have morphological  
577 data of their tentacles. While the limited dataset used here is informative for generating  
578 tentative hypotheses, the empirical data are still scarce and insufficient to cast robust  
579 predictions. This reveals the need to extensively characterize siphonophore diets and feeding  
580 habits. In future work, we can test these ecological hypotheses and validate these models  
581 by directly characterizing the diets of some of those siphonophore species. Predicting diet  
582 using morphology is a powerful tool to reconstruct food web topologies from community  
583 composition alone. In many of the ecological models found in the literature, interactions  
584 among the oceanic zooplankton have been treated as a black box (Mitra 2009). The ability  
585 to predict such interactions, including those of siphonophores and their prey, will enhance  
586 the taxonomic resolution of nutrient flow models constructed from plankton community  
587 composition data.

588 *Phenotypic integration of siphonophore tentilla* – Tentillum characters, such as nema-  
589 tocysts, arose from the subfunctionalization of serial homologs (David et al. 2008). Serial  
590 homologs have shared genetic elements underlying their development, and are expected to  
591 have phylogenetic correlations (Wagner and Schwenk 2000). In addition, these sub-structures  
592 must fit and work together in synchrony to ensnare prey successfully (functional integration).  
593 Character complexes that satisfy these conditions tend to be phenotypically integrated.  
594 Phenotypic integration is the set of functional and genetic correlations among the traits of an  
595 organism (Pigliucci 2003). These correlations have been hypothesized to direct and constrain  
596 adaptive evolution (Wagner and Schwenk 2000). The siphonophore tentillum morphospace  
597 has a fairly low extant dimensionality due to an evolutionary history with many synchronous,  
598 correlated changes. This is consistent with strong phenotypic integration where genetic and  
599 developmental correlations are maintained by natural selection to preserve function.

600 Part of the tentillum structural correlations are to be expected from shared regulatory

601 networks for elements that develop together from common positional bud (budding tentilla  
602 in the tentacle). Similarly, correlations between nematocyst subtypes are also expected  
603 given their common evolutionary and developmental origin. None of these explanations  
604 for correlated evolution are surprising, nor require natural selection. However, we also  
605 found correlations between nematocyst and tentillum characters. Siphonophore tentacle  
606 nematocysts (in their cnidocytes) are not produced nor matured in the developing tentillum.  
607 These cnidocytes are produced by dividing cnidoblasts in the basigaster (basal swelling  
608 of the gastrozooid). Once the cnidocytes have assembled the nematocyst, they migrate  
609 outward along the tentacle (Carré 1972) and position themselves in the tentillum according  
610 to their type and size (Skaer 1988). Thus, the developmental programs that produce the  
611 observed nematocyst morphologies are spatially separated from those producing the tentillum  
612 morphologies. Therefore, we hypothesize the genetic correlations and phenotypic integration  
613 between tentillum and nematocyst characters are maintained through natural selection on  
614 separate regulatory networks, out of the necessity to work together and meet the spatial,  
615 mechanical, and functional constraints of their prey capture behavior.

616       *Evolutionary history of tentillum morphology* – This study produced the most speciose  
617 siphonophore molecular phylogeny to date, while incorporating the most recent findings in  
618 siphonophore deep node relationships. This revealed for the first time that *Erenna* is the sister  
619 to *Stephanomia amphytridis*. *Erenna* and *Stephanomia* bear the largest tentilla among all  
620 siphonophores, thus their monophyly indicates that there was a single evolutionary transition  
621 to giant tentilla. Siphonophore tentilla range in size from ~30 µm in some *Cordagalma*  
622 specimens to 2-4 cm in *Erenna* species, and up to 8 cm in *Stephanomia amphytridis* (Pugh  
623 and Baxter 2014). Most siphonophore tentilla measure between 175 and 1007 µm (1st and  
624 3rd quartiles), with a median of 373 µm. The extreme gain of tentillum size in this newly  
625 found clade may have important implications for access to large prey size classes.

626       Tentillum size, as well as the majority of the characters studied, supported BM evolutionary  
627 models. There are two alternative hypotheses about the generative process of BM. One

628 hypothesis would suggest that these characters are not under selection, and therefore diverging  
629 neutrally (Lande 1976). The second hypothesis suggests that they are under selection, but  
630 the adaptive landscape was rapidly shifting (Hansen and Martins 1996), without leaving  
631 clear patterns across the phylogeny. Some of the BM supported characters are likely to have  
632 evolved under the second hypothesis, since when a diet-driven regime tree was provided,  
633 these characters preferentially supported an OU model (Appendix 14).

634 Siphonophore tentilla are defined as lateral, monostichous evaginations of the tentacle  
635 gastrovascular lumen with epidermal nematocysts (Totton and Bargmann 1965). The buttons  
636 on *Physalia* tentacles were not traditionally regarded as tentilla, but (Bardi and Marques  
637 2007) and our observations (Munro et al. 2018), confirm that the buttons contain evaginations  
638 of the gastrovascular lumen, thus satisfying all the criteria for the definition. In this light,  
639 and given that most Cystonectae bear conspicuous tentilla, we conclude (in agreement with  
640 (Munro et al. 2018)) that tentilla are likely ancestral to all siphonophores, and secondarily  
641 lost in *Apolemia* and *Bathyphysa conifera*.

642 The clade Tendiculophora contains far more species than its relatives Cystonectae, Apolemi-  
643 idae, and Pyrostephidae. An increase in clade richness and ecological diversification can be  
644 triggered by a ‘key innovation’ (Simpson 1955). The evolutionary innovation of the Tendicu-  
645 lophora tentilla with shooting cnidobands and modular regions may have facilitated further  
646 dietary diversification to unfold. In addition, our work identifies an interesting example of  
647 convergent evolution. The calycophoran tentillum morphospace (Fig. 9) was independently  
648 occupied by the physonect *Frillagalma vityazi*. Like calycophorans, *Frillagalma* tentilla have  
649 small C-shaped cnidobands with a few rows of anisorhizas. Unlike calycophorans, they lack  
650 paired elongate microbasic mastigophores. Instead, they bear three elongated stenoteles, and  
651 their cnidobands are followed by a branched vesicle, unique to this genus. Their tentillum  
652 morphology is very different from that of other related physonects, which tend to have long,  
653 coiled, cnidobands with many paired oval stenoteles. Most calycophoran diet studies have  
654 reported their prey to be small crustaceans such as copepods or ostracods. The diet of

655 *Frillagalma vityazi* is unknown, but this morphological convergence presents the hypothesis  
656 that they evolved to capture similar kinds of prey. Our DAPCs predict that *Frillagalma* has  
657 a generalist niche with both soft and hard bodied prey, including copepods.

658 *Evolution of nematocyst shape* – The phylogenetic placement of siphonophores among  
659 the Hydrozoa remains an unresolved question (Munro et al. 2018). The most recent  
660 work on this front sets them as sister group to all other Hydroidolina (Kayal et al. 2015).  
661 All reconstructions of hydrozoan relationships recover siphonophores as an early diverging  
662 lineage within Hydroidolina, with many unique apomorphic characters. Therefore, there  
663 is a great uncertainty around the ancestral plesiomorphies of the common ancestor of all  
664 siphonophores. This is especially true for those characters that present extreme differences  
665 between Cystonectae and Codonophora (the earliest split in the siphonophore phylogeny). One  
666 such character is the shape of haploneme nematocysts. A remarkable feature of siphonophore  
667 haplonemes is that they are outliers to all other Medusozoa in their surface area to volume  
668 relationships, deviating significantly from sphericity (Thomason 1988). This suggests a  
669 different mechanism for their discharge that could be more reliant on capsule tension than  
670 on osmotic potentials (Carré and Carré 1980), and strong selection for efficient nematocyst  
671 packing in the cnidoband (Thomason 1988; Skaer 1988). Our results show that Codonophora  
672 underwent a shift towards elongation and Cystonectae towards sphericity, assuming the  
673 common ancestor had an intermediate state. Since we know that the haplonemes of other  
674 hydrozoan outgroups are generally spheroid, it is more parsimonious to assume that cystonects  
675 retain this ancestral state. Later, we observe a return to more rounded (ancestral) haplonemes  
676 in *Erenna*, associated with a secondary gain of a piscivorous trophic niche, like that exhibited  
677 by cystonects.

678 Simultaneous with this shift in haploneme shape, heteroneme shape evolution also presents  
679 a single transition to elongation. In addition, the clade defined by the most recent common  
680 ancestor of *Agalma* and *Nanomia* shows an increased rate of divergence for heteroneme shape,  
681 spanning extremes (from oval *Nanomia* stenoteles to the elongate *Agalma okenii* stenoteles)

682 in relatively short evolutionary time. While cystonects do not bear heteronemes in their  
683 tentacles, *Physalia physalis* bears stenoteles in other zooids, hypothetically used for defense  
684 rather than for prey capture. These stenotele heteronemes are rounded like those found in  
685 pyrostephids and apolemiids, which is consistent with the story of a single transition leading  
686 to the elongated heteronemes in the stem of Tendiculophora.

687 The implications of these results to the evolution of nematocyst function suggests that an  
688 innovation in the discharge mechanism of haplonemes may have occurred during the main shift  
689 to elongation. Elongate nematocysts can be tightly packed into cnidobands. We hypothesize  
690 this may be a Tendiculophora lineage-specific adaptation to packing more nematocysts into a  
691 limited tentillum space, as suggested by (Skaer 1988). Tendiculophora is the most abundant,  
692 speciose, and diverse (ecologically and morphologically) clade of siphonophores, containing  
693 the clades Euphysonectae and Calycophorae. We hypothesize that this packing-efficient  
694 haploeme morphology may have been a key innovation leading to the diversification of this  
695 clade. However, other characters that shifted concurrently in the stem of this clade may have  
696 been responsible for their extant diversity.

697 Some siphonophore clades have more nematocyst types than others in the tentacles  
698 (Tendiculophora has 4 types, Cystonectae and Apolemiidae have 1), or different subtypes  
699 (e.g. stenoteles, mastigophores, birhopaloids). Siphonophores bear nematocysts in different  
700 parts of the colony (tentacles, gastrozooids, papons, palpacles, bracts, nectophores, and  
701 gonozooids) (Totton and Bargmann 1965). In this paper we only look at the presence of  
702 nematocyst types in the tentacles, therefore the gains and losses reported are not necessarily  
703 morphological innovations, but developmental allocations. For instance, stenoteles (a type of  
704 heteroneme) are absent from the tentacles of *Physalia* and seem to reappear in Euphysonectae,  
705 but we know that *Physalia* has stenoteles in other body parts (Totton and Bargmann 1965).  
706 Nonetheless, siphonophores have evolved unique nematocyst types and subtypes, not present  
707 in any other cnidarian, such as the two types of rhopalonemes (acrophores and anacrophores),  
708 and the haploneme homotrichous anisorhizas (Werner 1965). Both these nematocyst types

709 evolved in the stem to Tendiculophora, and are likely morphological innovations, since they  
710 have not been yet found in any other tissue of any other organism. The gain of extreme  
711 elongation in the haplonemes of Tendiculophora can be interpreted as part of the character  
712 shift to a novel anisorhiza subtype.

713     *Diversity of discharge dynamics* – A fundamental corollary in functional morphology is  
714 that structural morphology determines functional performance (Wainwright and Reilly 1994).  
715 We expected the discharge dynamics exhibited by siphonophore tentilla should vary with their  
716 morphological diversity. Our results are consistent with this expectation, and we observe,  
717 for example, that cnidoband size largely correlates with cnidoband discharge speed. This  
718 suggests that prey escape response speed may determine the minimum cnidoband length for  
719 successful capture.

720     *Insights from tentillum morphology* – The measurements taken illustrate that the morpho-  
721 logical diversity of siphonophore tentilla and nematocysts spans clades, from the overall shape  
722 and size, to the dimensions of the nematocysts. Siphonophores bear the largest nematocysts  
723 among Hydrozoans, and present a wide variety of nematocyst sizes within the clade. The  
724 largest nematocysts in our dataset (*Bargmannia lata* by volume and *Resomia dunni* by  
725 length), are the largest of all nematocysts reported for cnidarians, and therefore possibly the  
726 largest intracellular organelles among all living things.

727     In addition to the insights produced in this study, the newly collected morphological  
728 data provide a unique resource for future studies, and a reference dataset for siphonophore  
729 identification. Many conspicuous categorical characters in siphonophore tentilla are very  
730 diagnostic, such as: the fluorescent lures of *Resomia ornicephala*, the bioluminescent lures  
731 of *Erenna* species, the unique branched vesicle of *Frillagalma vityazi*, the buoyant medusa-  
732 resembling vesicle of *Lychnagalma* with 8 pseudo-tentacles, the zig-zag morphology of *Resomia*  
733 species, the inverted orientation of *Physophora* cnidobands, the button-like tentilla of *Physalia*,  
734 or the acorn-shaped minute tentilla of *Cordagalma* species (Fig. 7). Some categorical  
735 characters are synapomorphic diagnostic characters for large clades, such as the proximal

<sup>736</sup> tentillum heteronemes of Eucladophora, the elastic strand, rhopalonemes, and desmonemes of  
<sup>737</sup> Tendiculophora, the larval tentilla of Euphysonectae, the two-sized isorhizas of Cystonectae,  
<sup>738</sup> the saccus canal of Pyrostephidae, or the seven rows of anisorrhizas in Calycophorae. These  
<sup>739</sup> characters should be used together with the classical nectophore and bract characters to  
<sup>740</sup> identify species or at least impute phylogenetic affiliation from incomplete material.

## <sup>741</sup> **Conclusions**

<sup>742</sup> Siphonophores have diverse predatory niches in the open ocean, ranging from mid-trophic  
<sup>743</sup> small crustacean eaters to piscivorous super-carnivores. With the evolution of diversified  
<sup>744</sup> prey type specializations comes the evolution of morphologies adapted to the challenges  
<sup>745</sup> posed by different prey. The results presented here indicate that the associations found  
<sup>746</sup> between siphonophore tentilla and their prey are a product of correlated evolution in highly  
<sup>747</sup> integrated traits. While much of the literature focuses on how predatory generalists evolve  
<sup>748</sup> into predatory specialists, in siphonophores we find predatory specialists can evolve into  
<sup>749</sup> generalists, and that specialists on one prey type have directly evolved into specialists on  
<sup>750</sup> other prey types. Our extended morphological characterization shows that the relationships  
<sup>751</sup> between form and ecology hold across a large set of taxa and characters, and can be used to  
<sup>752</sup> generate hypotheses on the feeding habits of uncharacterized species. We conclude that the  
<sup>753</sup> siphonophores were able to establish as abundant oceanic predators by occupying a variety of  
<sup>754</sup> trophic niches facilitated by the evolution and diversification of extraordinary prey capture  
<sup>755</sup> tools on their tentacles.

## <sup>756</sup> **Supplementary Materials**

<sup>757</sup> Data available from the Dryad Digital Repository: <http://dx.doi.org/10.5061/dryad.NNNN>  
<sup>758</sup> Online Appendices are available in [https://github.com/dunnlab/tentilla\\_morph/](https://github.com/dunnlab/tentilla_morph/)  
<sup>759</sup> Supplementary\_materials/Online\_Appendices

760 **Funding**

761 This work was supported by the Society of Systematic Biologists (Graduate Student Award  
762 to A.D.S.); the Yale Institute of Biospheric Studies (Doctoral Pilot Grant to A.D.S.); and  
763 the National Science Foundation (Waterman Award to C.W.D., and NSF-OCE 1829835 to  
764 C.W.D., S.H.D.H., and C. Anela Choy). A.D.S. was supported by a Fulbright Spain Graduate  
765 Studies Scholarship.

766 **Acknowledgements**

767 We wish to thank the crew and scientists of the R/V Western Flyer, who participated in  
768 the collection of many of the specimens used in this study. We also want to thank Lynne  
769 Christianson and Shannon Johnson from the Monterey Bay Aquarium Research Institute  
770 for their assistance in the field as well as for sequencing some of the species included in this  
771 phylogeny. In addition, we wish to thank Lourdes Rojas, Daniel Drew, and Eric Lazo-Wasem  
772 for their assistance in imaging the fixed specimens and managing the collections. We thank  
773 Dennis Pilarczyk for organizing the prey selectivity data, and Joaquin Nunez for reviewing  
774 this manuscript. Furthermore, we thank Elizabeth D. Hetherington and C. Anela Choy  
775 for collating the data on siphonophore feeding and for reviewing the manuscript. Finally,  
776 we thank Philip Pugh, who confirmed many of our specimen identifications and taught us  
777 valuable knowledge about siphonophores.

778 **References**

- 779 Adams D.C., Collyer M., Kaliontzopoulou A., Sherratt E. 2016. Geomorph: Software for  
780 geometric morphometric analyses..
- 781 Andersen O.G.N. 1981. Redescription of marrus orthocanna (kramp, 1942)(Cnidaria,  
782 siphonophora). Zoological Museum, University of Copenhagen.
- 783 Bardi J., Marques A.C. 2007. Taxonomic redescription of the portuguese man-of-war,

- 784 physalia physalis (cnidaria, hydrozoa, siphonophorae, cystonectae) from brazil. Iheringia.  
785 Série Zoologia. 97:425–433.
- 786 Beaulieu J., O'Meara B. 2012. OUwie: Analysis of evolutionary rates in an ou framework.  
787 R package version 1.17..
- 788 Biggs D.C. 1977. Field studies of fishing, feeding, and digestion in siphonophores. Marine  
789 & Freshwater Behaviour & Phy. 4:261–274.
- 790 Blomberg S.P., Garland T., Ives A.R. 2003. Testing for phylogenetic signal in comparative  
791 data: Behavioral traits are more labile. Evolution. 57:717–745.
- 792 Blyth C.R. 1972. On simpson's paradox and the sure-thing principle. Journal of the  
793 American Statistical Association. 67:364–366.
- 794 Butler M.A., King A.A. 2004. Phylogenetic comparative analysis: A modeling approach  
795 for adaptive evolution. The American Naturalist. 164:683–695.
- 796 Carré D. 1972. Study on development of cnidocysts in gastrozooids of muggiaeae kochi  
797 (will, 1844) (siphonophora, calycophora). Comptes Rendus Hebdomadaires des Seances de  
798 l'Academie des Sciences Serie D. 275:1263.
- 799 Carré D., Carré C. 1980. On triggering and control of cnidocyst discharge. Marine &  
800 Freshwater Behaviour & Phy. 7:109–117.
- 801 Choy C.A., Haddock S.H., Robison B.H. 2017. Deep pelagic food web structure as revealed  
802 by in situ feeding observations. Proceedings of the Royal Society B: Biological Sciences.  
803 284:20172116.
- 804 Collins T.J. 2007. ImageJ for microscopy. Biotechniques. 43:S25–S30.
- 805 Costello J.H., Colin S.P., Gemmell B.J., Dabiri J.O., Sutherland K.R. 2015. Multi-jet  
806 propulsion organized by clonal development in a colonial siphonophore. Nature communica-  
807 tions. 6:8158.
- 808 Cressler C.E., Butler M.A., King A.A. 2015. Detecting adaptive evolution in phylogenetic  
809 comparative analysis using the ornstein–uhlenbeck model. Systematic biology. 64:953–968.
- 810 David C.N., Özbek S., Adamczyk P., Meier S., Pauly B., Chapman J., Hwang J.S.,

- 811 Gojobori T., Holstein T.W. 2008. Evolution of complex structures: Minicollagens shape the  
812 cnidarian nematocyst. *Trends in genetics.* 24:431–438.
- 813 Dunn C.W., Pugh P.R., Haddock S.H. 2005. Molecular phylogenetics of the siphonophora  
814 (cnidaria), with implications for the evolution of functional specialization. *Systematic biology.*  
815 54:916–935.
- 816 Felsenstein J. 1985. Phylogenies and the comparative method. *The American Naturalist.*  
817 125:1–15.
- 818 Futuyma D.J., Moreno G. 1988. The evolution of ecological specialization. *Annual review*  
819 *of Ecology and Systematics.* 19:207–233.
- 820 Grafen A. 1989. The phylogenetic regression. *Philosophical Transactions of the Royal*  
821 *Society of London. B, Biological Sciences.* 326:119–157.
- 822 Haddock S.H., Dunn C.W. 2015. Fluorescent proteins function as a prey attractant:  
823 Experimental evidence from the hydromedusa olindias formosus and other marine organisms.  
824 *Biology open.* 4:1094–1104.
- 825 Haddock S.H., Dunn C.W., Pugh P.R., Schnitzler C.E. 2005. Bioluminescent and red-  
826 fluorescent lures in a deep-sea siphonophore. *Science.* 309:263–263.
- 827 Haddock S.H., Heine J.N. 2005. Scientific blue-water diving. California Sea Grant College  
828 Program.
- 829 Hansen T.F., Martins E.P. 1996. Translating between microevolutionary process and  
830 macroevolutionary patterns: The correlation structure of interspecific data. *Evolution.*  
831 50:1404–1417.
- 832 Hardin G. 1960. The competitive exclusion principle. *science.* 131:1292–1297.
- 833 Harmon L.J., Losos J.B., Jonathan Davies T., Gillespie R.G., Gittleman J.L., Bryan  
834 Jennings W., Kozak K.H., McPeek M.A., Moreno-Roark F., Near T.J., others. 2010. Early  
835 bursts of body size and shape evolution are rare in comparative data. *Evolution: International*  
836 *Journal of Organic Evolution.* 64:2385–2396.
- 837 Harmon L.J., Weir J.T., Brock C.D., Glor R.E., Challenger W. 2007. GEIGER: Investi-

- 838 gating evolutionary radiations. *Bioinformatics*. 24:129–131.
- 839     Hessinger D.A. 1988. Nematocyst venoms and toxins. *The biology of nematocysts*.  
840     Elsevier. p. 333–368.
- 841     Hissmann K. 2005. In situ observations on benthic siphonophores (physonectae: Rhodali-  
842     idae) and descriptions of three new species from indonesia and south africa. *Systematics and*  
843     *Biodiversity*. 2:223–249.
- 844     Hoberg E.P., Brooks D.R. 2008. A macroevolutionary mosaic: Episodic host-switching,  
845     geographical colonization and diversification in complex host–parasite systems. *Journal of*  
846     *Biogeography*. 35:1533–1550.
- 847     Höhna S., Landis M.J., Heath T.A., Boussau B., Lartillot N., Moore B.R., Huelsenbeck  
848     J.P., Ronquist F. 2016. RevBayes: Bayesian phylogenetic inference using graphical models  
849     and an interactive model-specification language. *Systematic Biology*. 65:726–736.
- 850     Hutchinson G.E. 1961. The paradox of the plankton. *The American Naturalist*. 95:137–  
851     145.
- 852     Jacobs J. 1974. Quantitative measurement of food selection. *Oecologia*. 14:413–417.
- 853     Johnson K.P., Malenke J.R., Clayton D.H. 2009. Competition promotes the evolution of  
854     host generalists in obligate parasites. *Proceedings of the Royal Society B: Biological Sciences*.  
855     276:3921–3926.
- 856     Jombart T., Devillard S., Balloux F. 2010. Discriminant analysis of principal components:  
857     A new method for the analysis of genetically structured populations. *BMC genetics*. 11:94.
- 858     Kalyaanamoorthy S., Minh B.Q., Wong T.K., Haeseler A. von, Jermiin L.S. 2017. Mod-  
859     elFinder: Fast model selection for accurate phylogenetic estimates. *Nature methods*. 14:587.
- 860     Katoh K., Misawa K., Kuma K.-i., Miyata T. 2002. MAFFT: A novel method for  
861     rapid multiple sequence alignment based on fast fourier transform. *Nucleic acids research*.  
862     30:3059–3066.
- 863     Kayal E., Bentlage B., Cartwright P., Yanagihara A.A., Lindsay D.J., Hopcroft R.R.,  
864     Collins A.G. 2015. Phylogenetic analysis of higher-level relationships within hydroidolina

- 865 (cnidaria: Hydrozoa) using mitochondrial genome data and insight into their mitochondrial  
866 transcription. PeerJ. 3:e1403.
- 867 Lande R. 1976. Natural selection and random genetic drift in phenotypic evolution.  
868 Evolution. 30:314–334.
- 869 Longhurst A.R. 1985. The structure and evolution of plankton communities. Progress in  
870 Oceanography. 15:1–35.
- 871 Mackie G.O., Pugh P.R., Purcell J.E. 1987. Siphonophore Biology. Advances in Marine  
872 Biology. 24:97–262.
- 873 Mapstone G.M. 2014. Global diversity and review of siphonophorae (cnidaria: Hydrozoa).  
874 PLoS One. 9:e87737.
- 875 Martins E.P. 1996. Phylogenies, spatial autoregression, and the comparative method: A  
876 computer simulation test. Evolution. 50:1750–1765.
- 877 Mitra A. 2009. Are closure terms appropriate or necessary descriptors of zooplankton loss  
878 in nutrient–phytoplankton–zooplankton type models? Ecological Modelling. 220:611–620.
- 879 Munro C., Siebert S., Zapata F., Howison M., Serrano A.D., Church S.H., Goetz F.E.,  
880 Pugh P.R., Haddock S.H., Dunn C.W. 2018. Improved phylogenetic resolution within  
881 siphonophora (cnidaria) with implications for trait evolution. Molecular Phylogenetics and  
882 Evolution.
- 883 Nguyen L.-T., Schmidt H.A., Haeseler A. von, Minh B.Q. 2014. IQ-tree: A fast and  
884 effective stochastic algorithm for estimating maximum-likelihood phylogenies. Molecular  
885 biology and evolution. 32:268–274.
- 886 O’Brien T.D. 2007. COPEPOD, a global plankton database: A review of the 2007  
887 database contents and new quality control methodology..
- 888 Pagel M. 1994. Detecting correlated evolution on phylogenies: A general method for the  
889 comparative analysis of discrete characters. Proceedings of the Royal Society of London.  
890 Series B: Biological Sciences. 255:37–45.
- 891 Paradis E., Blomberg S., Bolker B., Brown J., Claude J., Cuong H.S., Desper R. 2019.

- 892 Package “ape”. Analyses of phylogenetics and evolution, version.:2–4.
- 893 Pennell M.W., FitzJohn R.G., Cornwell W.K., Harmon L.J. 2015. Model adequacy and
- 894 the macroevolution of angiosperm functional traits. *The American Naturalist*. 186:E33–E50.
- 895 Pigliucci M. 2003. Phenotypic integration: Studying the ecology and evolution of complex
- 896 phenotypes. *Ecology Letters*. 6:265–272.
- 897 Pugh P. 2001. A review of the genus *erenna bedot*, 1904 (siphonophora, physonectae).
- 898 BULLETIN-NATURAL HISTORY MUSEUM ZOOLOGY SERIES. 67:169–182.
- 899 Pugh P., Baxter E. 2014. A review of the physonect siphonophore genera *halistemma*
- 900 (family agalmatidae) and *stephanomia* (family stephanomiidae). *Zootaxa*. 3897:1–111.
- 901 Pugh P., Youngbluth M. 1988. Two new species of prayine siphonophore (calycophorae,
- 902 prayidae) collected by the submersibles johnson-sea-link i and ii. *Journal of Plankton Research*.
- 903 10:637–657.
- 904 Purcell J. 1981. Dietary composition and diel feeding patterns of epipelagic siphonophores.
- 905 *Marine Biology*. 65:83–90.
- 906 Purcell J.E. 1980. Influence of siphonophore behavior upon their natural diets: Evidence
- 907 for aggressive mimicry. *Science*. 209:1045–1047.
- 908 Purcell J.E. 1984. The functions of nematocysts in prey capture by epipelagic
- 909 siphonophores (coelenterata, hydrozoa). *The Biological Bulletin*. 166:310–327.
- 910 Purcell J., Mills C. 1988. The correlation of nematocyst types to diets in pelagic hydrozoa.
- 911 In “the biology of nematocysts”.(Eds da hessinger and hm lenhoff.) pp. 463–485..
- 912 Rabosky D.L., Grunbler M., Anderson C., Title P., Shi J.J., Brown J.W., Huang H.,
- 913 Larson J.G. 2014. BAMM tools: An r package for the analysis of evolutionary dynamics on
- 914 phylogenetic trees. *Methods in Ecology and Evolution*. 5:701–707.
- 915 Revell L.J. 2012. Phytools: An r package for phylogenetic comparative biology (and other
- 916 things). *Methods in Ecology and Evolution*. 3:217–223.
- 917 Revell L.J., Chamberlain S.A. 2014. Rphylip: An r interface for phylip. *Methods in*
- 918 *Ecology and Evolution*. 5:976–981.

- 919 Robison B.H. 2004. Deep pelagic biology. *Journal of experimental marine biology and*  
920 *ecology.* 300:253–272.
- 921 Schindelin J., Arganda-Carreras I., Frise E., Kaynig V., Longair M., Pietzsch T., Preibisch  
922 S., Rueden C., Saalfeld S., Schmid B., others. 2012. Fiji: An open-source platform for  
923 biological-image analysis. *Nature methods.* 9:676.
- 924 Schluter D. 2000. Ecological character displacement in adaptive radiation. *the american*  
925 *naturalist.* 156:S4–S16.
- 926 Schmitz O. 2017. Predator and prey functional traits: Understanding the adaptive  
927 machinery driving predator–prey interactions. *F1000Research.* 6.
- 928 Shapiro S.S., Wilk M.B. 1965. An analysis of variance test for normality (complete  
929 samples). *Biometrika.* 52:591–611.
- 930 Siebert S., Pugh P.R., Haddock S.H., Dunn C.W. 2013. Re-evaluation of characters in  
931 apolemidae (siphonophora), with description of two new species from monterey bay, california.  
932 *Zootaxa.* 3702:201–232.
- 933 Simpson G.G. 1944. *Tempo and mode in evolution.* Columbia University Press.
- 934 Simpson G.G. 1955. *Major features of evolution.* Columbia University Press: New York.
- 935 Skaer R. 1988. The formation of cnidocyte patterns in siphonophores. Academic Press  
936 New York.
- 937 Skaer R. 1991. Remodelling during the development of nematocysts in a siphonophore.  
938 *Hydrobiologia.* 216:685–689.
- 939 Stireman-III J.O. 2005. The evolution of generalization? Parasitoid flies and the perils of  
940 inferring host range evolution from phylogenies. *Journal of evolutionary biology.* 18:325–336.
- 941 Sugiura N. 1978. Further analysts of the data by akaike's information criterion and the  
942 finite corrections: Further analysts of the data by akaike's. *Communications in Statistics-*  
943 *Theory and Methods.* 7:13–26.
- 944 Team R.C. 2017. R: A language and environment for statistical computing. Vienna,  
945 austria: R foundation for statistical computing; 2017..

- 946        Thomason J. 1988. The allometry of nematocysts. *The biology of nematocysts*. Elsevier.
- 947        p. 575–588.
- 948        Totton A.K., Bargmann H.E. 1965. A synopsis of the siphonophora. *British Museum*
- 949        (Natural History).
- 950        Uhlenbeck G.E., Ornstein L.S. 1930. On the theory of the brownian motion. *Physical*
- 951        review. 36:823.
- 952        Uyeda J.C., Zenil-Ferguson R., Pennell M.W. 2018. Rethinking phylogenetic comparative
- 953        methods. *Systematic Biology*. 67:1091–1109.
- 954        Wagner G.P., Schwenk K. 2000. Evolutionarily stable configurations: Functional in-
- 955        tegration and the evolution of phenotypic stability. *Evolutionary biology*. Springer. p.
- 956        155–217.
- 957        Wainwright P.C., Reilly S.M. 1994. *Ecological morphology: Integrative organismal biology*.
- 958        University of Chicago Press.
- 959        Werner B. 1965. Die nesselkapseln der cnidaria, mit besonderer berücksichtigung der
- 960        hydriida. *Helgoländer wissenschaftliche Meeresuntersuchungen*. 12:1.